

The Nature and Geometry of the Hanaupah Fault, Panamint
Mountains, Death Valley, California

Gabriel Cisneros

A thesis submitted in partial fulfillment of the requirements for the degree of

Master of Science

University of Washington

2002

Program authorized to offer degree

Department of Earth and Space Sciences

University of Washington
Graduate School

This is to certify that I have examined this copy of a master's thesis by

Gabriel Cisneros

And have found that it is complete and satisfactory in all respects,
and that any and all revisions required by the final
examining committee have been made.

Committee Members:

Darrel Cowan

Darrel Cowan

Ralph Haugerud

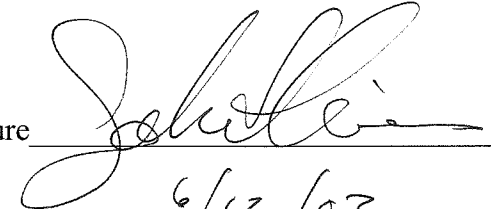
Ralph Haugerud

Date:

12 June 2002

In presenting this thesis in partial fulfillment of the requirements for a Master's degree at the University of Washington, I agree that the Library shall make its copies freely available for inspection. I further agree that extensive copying of this thesis is allowable only for scholarly purposes, consistent with "fair use" as prescribed in the U.S. Copyright Law. Any other reproduction for any purposes or by any means shall not be allowed without my written permission.

Signature

A handwritten signature in cursive script, appearing to read "John L. ...", written over a horizontal line.

Date

6/12/02

TABLE OF CONTENTS

	Page
List of Figures.....	ii
Introduction.....	1
Purpose.....	4
Methods.....	6
Geologic Setting.....	9
Stratigraphy of Rock Units.....	13
Footwall Rocks.....	15
Hanging-wall Rocks.....	17
Structural Geology of the Hanaupah Canyon Area.....	28
Footwall Structure.....	33
Hanging-wall Structure.....	39
Structural Interpretation.....	48
Fault Reconstruction.....	54
Age of the Hanaupah Detachment.....	60
Discussion and Conclusions.....	61
References Cited.....	64
Pocket Material: Plate 1	

LIST OF FIGURES

Figure Number	Page
1. Vicinity Map.....	2
2a. ASTER Satellite Image of Central Death Valley Region.....	7
2b. ASTER Satellite Image of Hanaupah Canyon Area.....	8
3. Stratigraphic Column.....	14
4. Photographs of Hanaupah Fault.....	16
5a. Cross Section A-A'.....	30
5b. Cross Section B-B'.....	31
5c. Cross Section C-C'.....	32
6. Photograph of Basement Rocks.....	34
7a/b. Photograph of Augen Gneiss.....	37
7c/d. Photograph of Augen Gneiss.....	38
8. Hanging-wall Normal Fault.....	40
9. Breccia Contact of Hanging-wall Normal Fault.....	41
10a. Hanging-wall Normal Fault.....	43
10b. Fault Gouge of a Normal Fault.....	44
11. Fault Scarp Cutting Alluvium.....	46
12. Extensional Duplex Model.....	50
13. Interpretive Cross Section Across A-A'.....	53
14a. Restored Cross Section Across A-A'.....	55
14b. Restored Cross Section Across B-B'.....	56
14c. Restored Cross Section Across C-C'.....	57

Acknowledgements

I wish to thank the Department of Earth and Space Sciences (ESS) for their support over the last three years at the University of Washington. I would like to thank the EDMAP program in funding my research in Death Valley. I greatly appreciate the friendly advice and support from other ESS graduate students. Without their support these last three years would not of gone as smoothly as they did. The following graduate students made a great impact on my social and learning experience: Nate Chutas, Nick Hayman, Chris Brummer, and Paul Zehfuss. I would like to thank Karen Sorensen for her faithful support, understanding, and patience with me over the last three years. I also greatly appreciate the support my parents, George and Barbara Cisneros, have giving over the years. Their love and understanding have helped me throughout the years and years to come,

I would like to express my sincere appreciation to my two thesis advisors, Ralph Haugerud and Darrel S. Cowan. I would like to thank Ralph Haugerud for spending endless hours with me in front of the computer teaching the ways of ArcInfo, being so supportive of my work, and his many comments, suggestions, and editing concerning my thesis. I would like to thank Darrel S. Cowan for being my thesis advisor and a friend. I could always count on him to answer my questions any time of the day without an advanced notice. I greatly appreciate his many questions, comments, suggestions, editing, and support concerning my thesis and non-thesis topics. Both Darrel and Ralph made my experience at University of Washington very enjoyable.

Dedication

I would like to dedicate my thesis to my family: George, Barbara, Teresa, Maria, Tristan, Maiya, Angel Cisneros, and Grandma Belen. I would also like to extend this dedication to Karen Sorensen. Without the love and support of them I would not be where I am today. Thank you.

The Nature and Geometry of the Hanaupah Fault, Panamint Mountains, Death Valley, California.

INTRODUCTION

The Death Valley region, southeastern California, has undergone large-scale extension since the Miocene (McKenna et al., 1990). Well-exposed geology and structures have made the Death Valley region important to the understanding of large-scale extension (Noble, 1941; Hunt and Mabey, 1966; Wright and Troxel, 1973; Wright, et al., 1974; Wernicke, 1988; Hamilton, 1988). Death Valley is bounded by the Panamint Mountains to the west and the Black Mountains to the east (Figure 1). Death Valley basin is presently a half-graben, in which the Panamint Mountains are exposed on the eastward tilted block.

There has been considerable debate concerning the age, sense of throw, and amount displacement on the normal fault systems in the Panamint Mountains. Early work by Hunt and Mabey (1966) revealed a fault system consisting of low-angle thrust and high-angle normal faults in the eastern side of the Panamint Range. They related these thrust faults to the contractional Amargosa thrust of Noble (1941). However, Hamilton (1988) renamed the most significant fault of the system the *Hanaupah* fault and interpreted it to have normal sense of slip. In his interpretation, the Hanaupah fault is a low-angle normal or detachment fault that dips westward below the Panamint Mountains. Based on field mapping, McKenna and Hodges (1990) later suggested that the Chuckwalla fault (same as Hamilton's Hanaupah fault, and for the remainder of my thesis

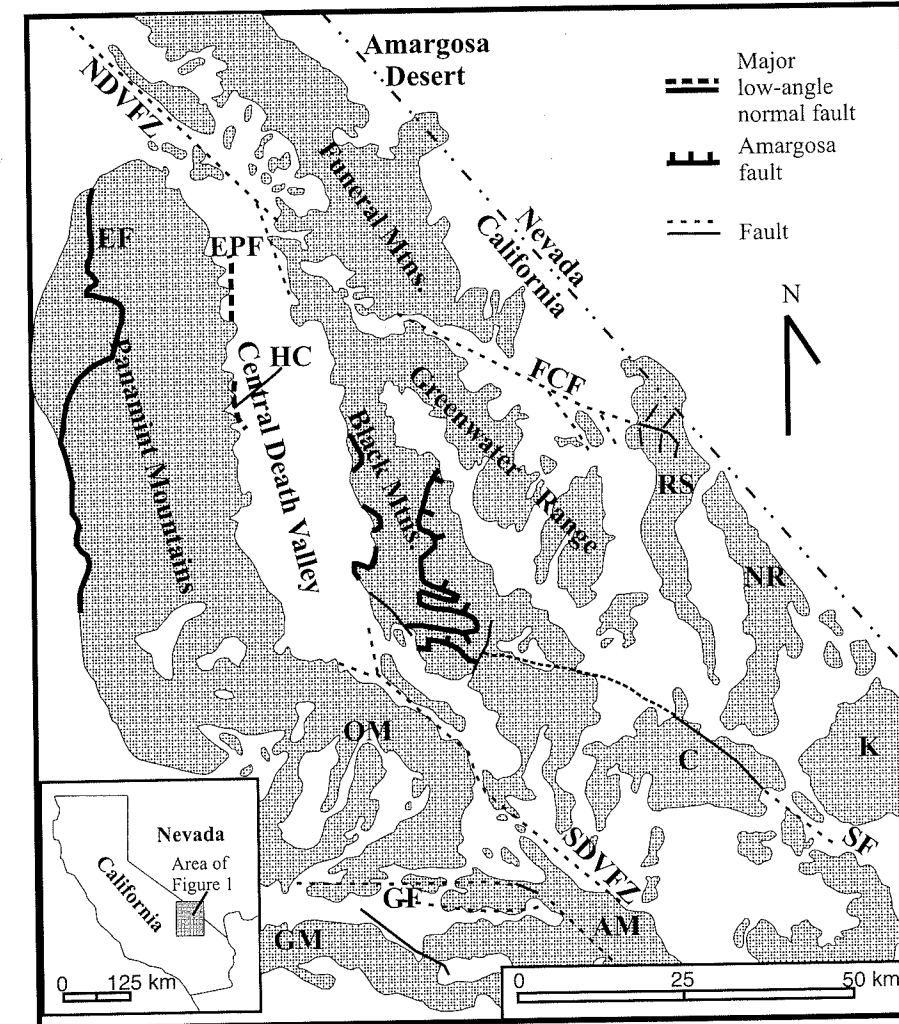


Figure 1. Map showing topographic features and faults of the central Death Valley region. Abbreviations: A, Avawatz Mountains; C, China Ranch/Sperry Hills Basin; EF, Emigrant fault; EPF, Eastern Panamint Fault; FCF, Furnace Creek fault zone; GF, Garlock fault zone; GM, Granite Mountains; HC, Hanaupah Canyon; K, Kingston Range; NR, Nopah Range; NDVFZ, Northern Death Valley fault zone; OM, Owshead Mountains; RS, Resting Spring Range; SF, Sheephead fault zone; SDVFZ, Southern Death Valley fault zone. Dashed lines represent buried structures (Modified from Wright et al., 1991).

I will use the name coined by Hamilton) has had only a few kilometers of slip, and that it is the basal fault of a rotated extensional duplex, which they named the *Eastern Panamint fault system*. Despite conflicting interpretations of the displacement and geometry of the Hanaupah fault, it remains clear that (1) the fault system is related to the Miocene and younger extension of the Death Valley region, because the fault system cuts Miocene volcanic rocks, and (2) the Death Valley region is related to large intra-continental extension (Hodges et al. 1990).

PURPOSE

The findings of McKenna and Hodges (1990) and Wernicke et al. (1988) changed our understanding of the tectonic history of the Panamint Mountains, and illustrate the crucial role of field research in interpreting the geology of the area. My own study uses the same approach, relying on detailed mapping to provide insights to fundamental questions about the Hanaupah fault. These questions include the following:

1. What is the sense of slip on the low-angle faults? Are they extensional or contractional? If any of the faults are contractional, does evidence exist that tells their age?
2. What are the relative ages of the steeply and gently dipping faults? Are the steeply dipping faults ramps and transfer faults, as suggested by McKenna and Hodges (1990)? Or are the lower-angle faults conventional high-angle faults that have been rotated from original dip angles? Do the high-angle faults in the footwall cut or intersect the Hanaupah fault?
3. What is the nature of the Hanaupah fault that juxtaposes Proterozoic and Paleozoic strata with crystalline basement? Can it be considered a detachment fault as proposed by Hamilton (1988)?
4. Does the Hanaupah fault exhibit mylonitic fabrics?
5. What is the amount of displacement on the Hanaupah fault? How does it compare with the overall stratigraphic throw on the fault system mapped by McKenna and Hodges, who proposed a minimum throw of 7 km? Is

the amount of throw in my study area compatible with Hamilton's proposal (1988) that the Hanaupah fault accommodated $\gg 7$ km of slip, in the eastern Panamint Mountains?

6. Is the eastern Panamint fault system still active?

In addition to these specific questions, this study will contribute to ongoing research concerning intra-continental extension, and my map and results will be useful to the worldwide community of scientists interested in the geology of the Death Valley region.

METHODS

I spent approximately forty days mapping, gathering structural data, and collecting samples in the region north of Hanaupah Canyon (Figure 2b). I mapped at scales of 1:12,000 and 1:24,000 using USGS topographic maps. During this time, I mapped Proterozoic and Lower Cambrian sedimentary rocks that constitute the hanging wall of a low-angle normal fault, as well as lower Proterozoic basement rocks that constitute the footwall. I collected samples of the footwall rocks and examined them in thin section, and submitted felsic dikes, in the footwall, for isotopic dating. I recorded small-scale structural measurements in the field, and collected representative structural measurements. I mapped the alluvial fans that drain from the Hanaupah Canyon into Death Valley, by recording lithology differences in the alluvium and using color aerial photographs at a 1:24,000 scale.

I scanned my field maps, registered the scans to DRGs (digital raster graphics) of the Hanaupah and Devil's Speedway 7.5-minute quadrangles, and digitized the scans on-screen using DIG (Digitizing Interface for Geologists), a set of Arc-Info export files for the resulting geologic map (units, contacts, and faults in one layer, strikes and dips in another) have been deposited with the EDMAP program of the U.S. Geological Survey. Please contact Peter Lyttle for copies of these files.

Haugerud assisted me in turning the Arc-Info files into a finished cartographic product (Plate 1). We merged geologic information with shaded relief topography and a DRG map base using the techniques outlined by Haugerud and Greenberg (1998).

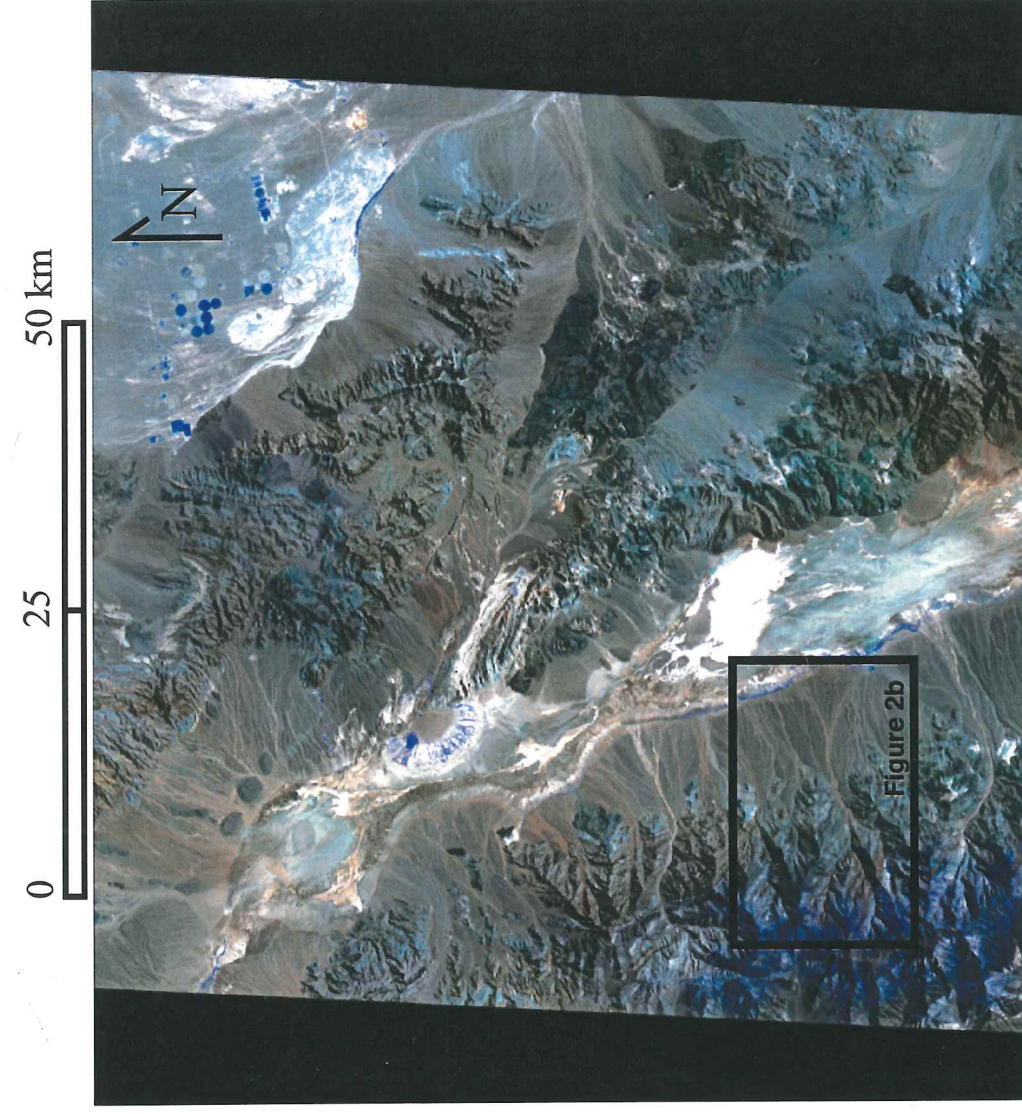


Figure 2a. ASTER satellite image of the central Death Valley region, provided by Alan Gillespie and Steve Thompson, UW Quaternary Research Center.

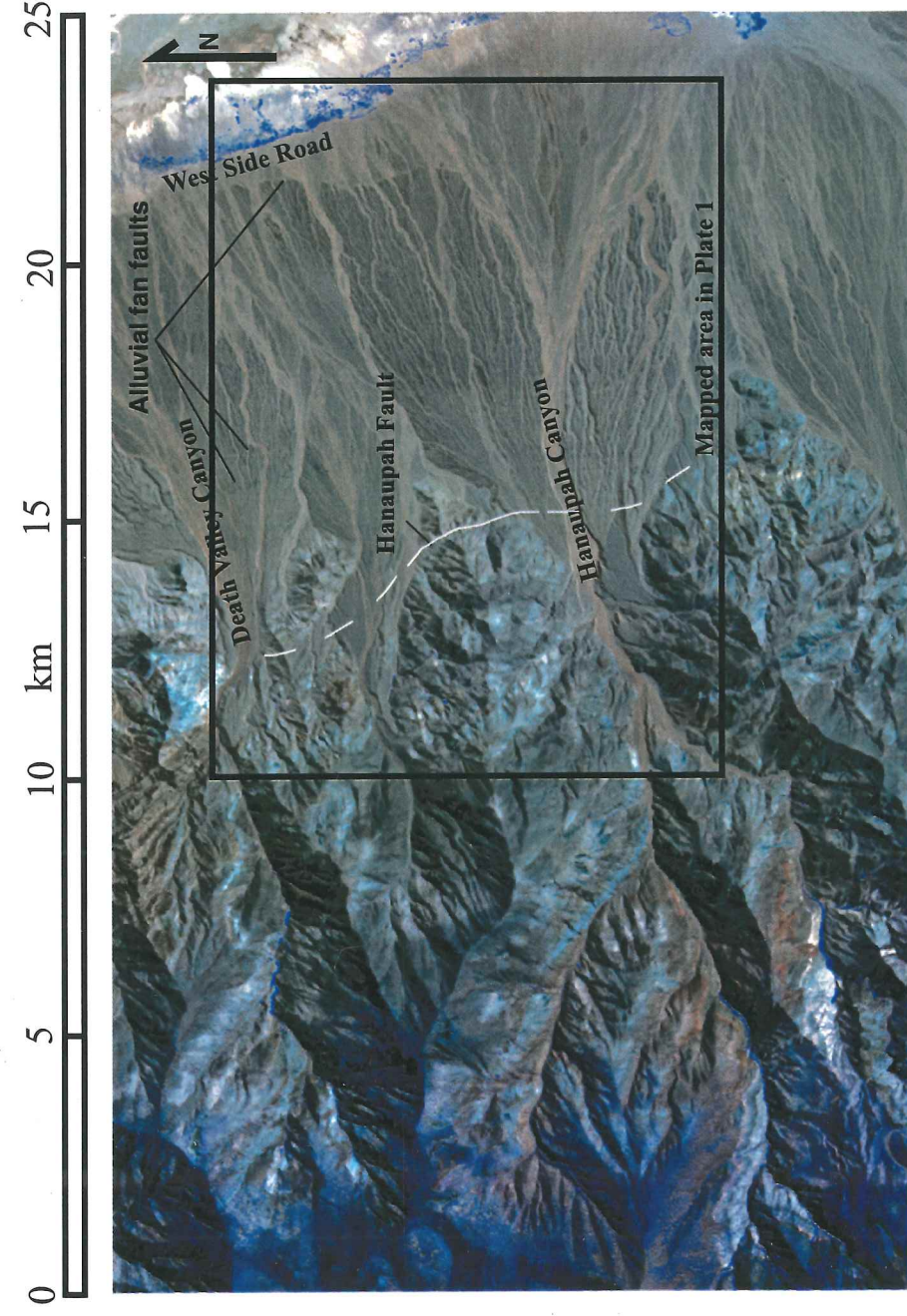


Figure 2b. ASTER satellite image of Hanaupah Canyon region. Boxed area shows the area mapped on Plate 1. Hanaupah fault is shown as a white line, and faults can be seen cutting the Pleistocene alluvium.

GEOLOGIC SETTING

Western North America is ideal for investigating large-scale intra-continental extension. The foremost region of extensional tectonism in western North America has been recognized for years as the Basin and Range Province (Stewart, 1978; Eaton, 1982). The Basin and Range Province includes the northern Basin and Range of Nevada and western Utah, the Arizona-Sonora Basin and Range of the southwestern United States and northwestern Mexico, and southeastern California. Throughout the Basin and Range region, much of the extension has been accommodated by low-angle detachment faults that are associated with metamorphic core complexes.

Metamorphic core complexes occur in a discontinuous belt extending from southern Canada south through the western Cordillera and into northwestern Mexico (Coney, 1980). Generally, all metamorphic core complexes exhibit similar characteristics, such as rock types, structures, and fabrics. Core complexes consist of basement rock composed of mylonitic augen gneiss, granodioritic rocks with screens of mylonitic schist, and metasedimentary and metavolcanic rocks or cataclastically deformed metasedimentary and metavolcanic rocks. Overlying these rocks is an unmetamorphosed cover. Separating the two is the detachment fault; a sharp discontinuous zone marking an abrupt change in rocks types, structure, and fabric. The structure, deformation, and fabric of the basement rock rarely cross over the fault zone into the cover rocks (Davis and Coney, 1979; Davis, 1980; Coney, 1980). These metamorphic core complexes are present throughout the Basin and Range Province and are well exposed in the Death Valley region.

The central Death Valley region (Figure 1) has opened by northwestward motion of the Panamint Mountains away from the Black Mountains (Burchfiel and Stewart, 1966). The extension was accommodated by a system of strike-slip and normal faults creating a "pull-apart basin" between the northwest-striking, right-lateral Northern Death Valley fault zone, Southern Death Valley fault zones, and oblique slip on a system of normal faults along the western flank of the Black Mountains (Burchfiel and Stewart, 1966; Wright and Troxel, 1967). Metamorphic core complexes are exposed both in the Black Mountains, as the turtlebacks (Wright et al., 1974; Burchfiel and Stewart, 1966; Asmerom, et al., 1990; Holm and Wernicke, 1990) and the Panamint Mountains (Labotka and others 1980; Labotka and Albee, 1990).

The Panamint Range bounds the west side of Death Valley. It is a north-trending range and is mainly composed of Precambrian rocks. Figure 1 is a map showing the Panamint Range in relation to surrounding ranges and faults in the Death Valley region. Figure 2a is an ASTER satellite image of the central Death Valley region featuring the Panamint, Black, and Funeral Mountains. The northern portion of the Panamint Mountains contains a domed core composed of upper Precambrian sedimentary rocks, granitic intrusive plutons, and numerous normal faults containing either Paleozoic sedimentary rocks or Plio-Pleistocene conglomerates in the hanging-wall (Hunt and Maybe, 1966; Labotka and Albee, 1990). The central portion of the Panamint Mountains contains the anticlinal World Beater dome of Precambrian rocks that are intruded by the Cretaceous Hall Canyon pluton and by the Miocene Little Chief stock (Hunt and Mabey, 1966; Labotka and Albee, 1990). In the southern part of the Panamints, the intrusion of

the Jurassic Manly Peak pluton deformed the Precambrian rocks making up the World Beater dome, and the South Park Canyon and Butte Valley faults juxtaposed the metamorphic core rocks of the Panamint Mountains with the Proterozoic gneisses, schists, and Paleozoic and Mesozoic sedimentary and volcanic rocks along the western margin of the southern Panamint Range (Labotka and Albee, 1990). Large-scale extension in the Panamint Mountains is evident throughout the range and is widely accepted (Hamilton, 1988; Wernicke et al., 1988; Labotka and Albee, 1990; McKenna and Hodges, 1990; Hodges et al., 1990), but how much extension has been accommodated by the Panamint Range?

Stewart (1983), Wernicke et al. (1988), Hamilton (1988), Topping (1993), and Brady et al. (2000) have suggested that the Panamint Range has moved more than 80 km to the northwest relative to the Nopah Range, and once was structurally situated above and east of the Black Mountains. On the other hand, Cemen et al. (1985), Wright et al. (1991), Serpa and Pavlis (1996), and Miller (2002) have proposed lesser amounts of regional extension. One goal of my thesis is to ascertain which model of extension is most compatible with my field observations.

My study area is located on the eastern side of the central Panamint Range and on the western side of Death Valley (Figures 2a and 2b). The southern boundary is Hanaupah Canyon, and the northern boundary is Death Valley Canyon. Elevations in the study area range from 282 ft below sea level to almost 4000 ft. The study area drains into Death Valley by east-sloping canyons and gullies. In the Hanaupah Canyon area, Proterozoic basement rocks are exposed along the eastern flank of the Panamint Range in

the footwall of a low-angle fault dipping to the west. Proterozoic and lower Cambrian rocks dipping to the east are exposed in the hanging wall of the detachment fault and are cut by several west-dipping, low-angle faults.

STRATIGRAPHY OF ROCK UNITS

Proterozoic and Cambrian rocks are widely exposed and well documented throughout the Death Valley Region (Hunt and Mabey, 1966, Hazzard, 1937). To become acquainted with the stratigraphy (of the area), I first visited and inspected these rocks in the southern Nopah Range, southeast of Death Valley. The southern Nopah Range is an excellent place to examine the Proterozoic and Cambrian rocks, of the Cordilleran miogeocline, because a full stratigraphic section from Noonday Dolomite to Bonanza King Formation is exposed.

In the Panamint Range, Proterozoic and lower Cambrian rocks, from the Noonday Dolomite to the Bonanza King Formation, are exposed on the east-facing slopes. A generalized stratigraphy is shown in Figure 3. I divided the Proterozoic and Early Cambrian units into lower, middle, and upper members for a more detailed definition of the stratigraphy, which enables better structural mapping. The older alluvial fans are composed of Pleistocene alluvium.

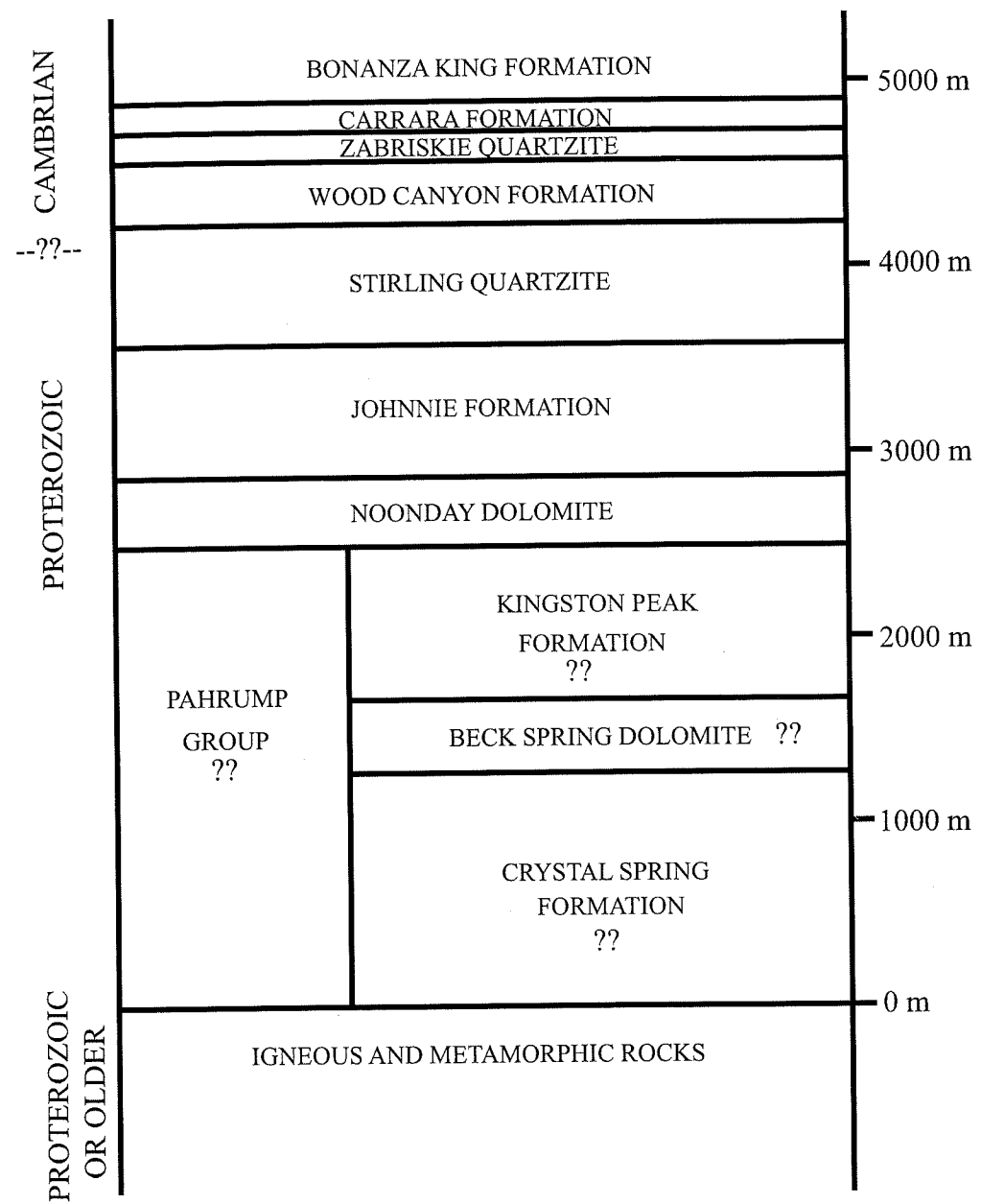


Figure 3. General stratigraphy of the Hanaupah Canyon region. Thickness of Pahrump Group taken from Miller, 1987b.

FOOTWALL ROCKS

Crystalline Basement (pC)

The oldest rocks within the field area are exposed in the footwall of the main detachment (the Hanaupah detachment fault) (Fig. 4). These rocks consist of augen gneiss, feldspar-biotite gneiss, muscovite schist, and quartz gneiss. The gneiss is medium to dark gray on fresh surfaces and weathers to reddish brown. The most abundant rock type of the footwall is the augen gneiss, which contains feldspar augens. The muscovite schist of the footwall contains foliation striking 140° and dipping 25° S. However, no lineations were evident. The augen gneiss does not appear to have the mylonitic fabric that is typical within the basement rocks of metamorphic core complexes (Davis, 1980; Davis and Coney, 1979; Armstrong, 1982). However, cataclastic deformation is present and increases upward toward the detachment fault in localized outcrops.

The gneiss is intruded by abundant silicic and intermediate Tertiary dikes, which range from a few centimeters to 2 meters wide. Contacts between the gneiss and dikes are sharp. The dikes are parallel, oriented sub-vertical and brecciated. However, Hamilton (1988) suggested that the dikes dip approximately 70° westward. In the field, I could not determine if the dikes had an overall dip of 70° westward. A more detailed field study on the dikes could be carried out that will determine if they are vertical or dipping to the west. The dikes are restricted to the footwall and do not cut rocks in the hanging wall.

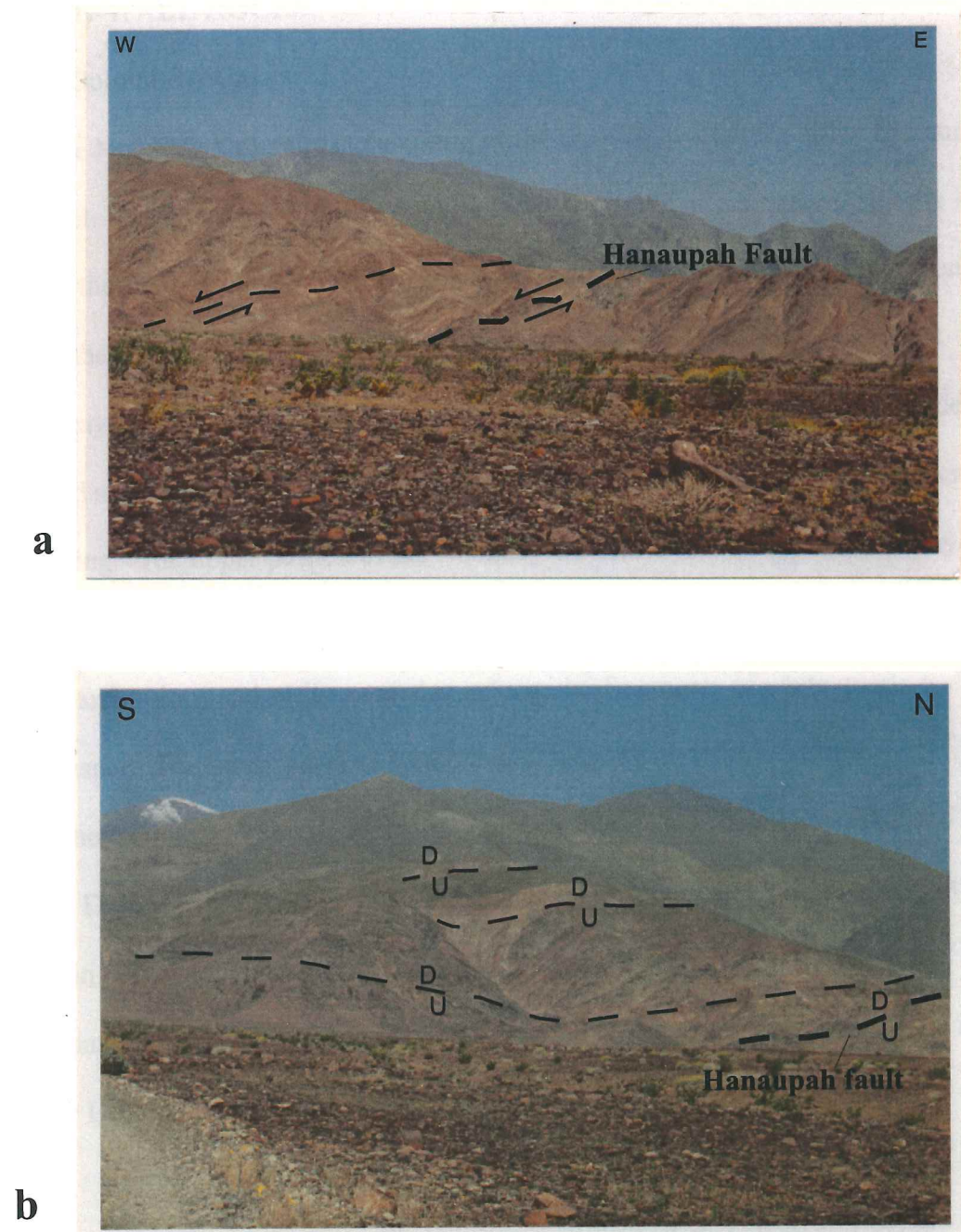


Figure 4. Photographs of the Hanaupah fault and hangingwall faults. Dashed lines mark faults. Movement of faults is represented by arrows and U (up) and D (down). **a:** Looking north from Hanaupah Canyon, footwall rocks consist of augen gneiss, and hanging-wall rocks consist of Stirling Quartzite. **b:** Looking west from Hanaupah Canyon road. The hanging-wall consists of Stirling Quartzite, Wood Canyon Formation, Zabriskie Quartzite, and low-angle faults dipping to the west. Telescope Peak is in the background.

HANGING-WALL ROCKS

Noonday Dolomite (pCn)

The Noonday Dolomite is the oldest of the hanging-wall rocks of the Hanaupah detachment. Only a sliver, 5 meters thick to 20 meters long, of Noonday Dolomite is present in the field area; however, it is abundant southwest of the Hanaupah Canyon area in the southern portion of the Panamint Range. The lower portion consists of light creamy-gray, fine-grained dolomite. The rock is typically massive and thinly bedded. Weathered surfaces of the dolomite are grayish yellow in color and the unit is generally cliff forming. The upper portion of the Noonday Dolomite consists of light creamy-gray, fine-grained to medium-grained sandy dolomite. It is generally poorly bedded and contains laminations and well-rounded to subangular fragments of white quartz and reddish jasper. The sandy portions weather to a rusty cream to brown color.

The Noonday Dolomite in the Hanaupah Canyon area roughly correlates to the Noonday Dolomite in the southern Nopah Range. The Noonday Dolomite was not fully exposed in the area that I mapped, but in the southern Panamint Range, it is approximately 330 m thick (Miller, 1987a; Miller, 1987b). No fossils were found in the Noonday Dolomite.

Johnnie Formation (pCj)

The Johnnie Formation in the study area is exposed in the southern section of the geologic map, just north of the Hanaupah wash. It can be divided into two members. The lower section consists of sandy dolomite and quartzite. The lower section contains

light gray to buff-colored layers from 20 cm to 10 m in thickness. Most of the dolomite is fine-grained and weathers to grayish brown. Some coarse-grained layers with well-rounded quartz pebbles are present. The upper portion of the Johnnie Formation is composed mostly of shale but contains abundant layers of fine-grained quartzite and a minor amount of fine-grained dolomite. The shale is predominantly brownish gray to greenish gray in the lower part, light brown and grayish orange in the middle, and maroon to grayish red in the upper part. Quartzite and dolomite vary in color from grayish brown to reddish brown.

The Johnnie Formation in the Hanaupah Canyon region is roughly similar to the Johnnie Formation in the southern Nopah Range. In the southern Panamint Range, it is approximately 600 to 700 m thick (Miller, 1987a). I mapped only a small portion of the upper member of the Johnnie Formation. However, a full section is exposed west of the area that was mapped. Using Hunt and Mabey's map (1966), I measured the Johnnie Formation at approximately 700 m in thickness. In the southern Nopah Range, the upper portion of this formation is marked by a resistant layer of oolitic dolomite about 2 m in thickness. This layer was not observed in the Hanaupah Canyon region but may be exposed in the southern Panamint Range. I did not find fossils in the Johnnie Formation. The contact between the Johnnie Formation and Stirling Quartzite is sharp and easily discernable. The lowest basal member of the Stirling Quartzite is composed of coarse-grained pebbly to cobbly sandstone and quartzite, which rests on greenish to reddish-gray shale of the upper Johnnie Formation

21121

Stirling Quartzite (pCs₁) lower quartzite member

In the Hanaupah Canyon area and in the southern Nopah Range the Stirling Quartzite can be divisible into three members. In the Panamint Range, I applied a three-fold division of the Stirling Quartzite, unlike Hunt and Mabey (1966), who mapped the Stirling Quartzite as one member. Dividing the Stirling Quartzite into three members produces a more detailed map. This highly detailed map leads to more accurate measurements of slip on faults within the Hanaupah Canyon area. The lower member of the Stirling Quartzite is composed of a dense, fine- to coarse-grained, well-sorted quartzite. It is generally light gray in color, but commonly tinted yellow, light red, and orange. The lower member is massively bedded and weathers to light reddish and various shades of brown. Beds average 1 meter in thickness, but platy layers and beds up to 2 meters in thickness exist. Abundant cross-beds are seen throughout the member, as well as well-developed ripple marks in the upper portion. Ripple marks can be used to distinguish the lower quartzite member from the upper quartzite member. The basal layer contains well-rounded quartz pebbles. Thinly bedded reddish and purplish-blue siliceous shale lenses are present throughout the lower member. At a distance the lower member appears massive and grayish to light reddish brown. It is highly resistant to erosion and typically a cliff former.

The lower member of the Stirling Quartzite in the Hanaupah Canyon area is very similar to the Stirling Quartzite in the southern Nopah Range. The lower member is displaced by faults and a full section is not observed in the mapped area. However, a whole section of the Stirling Quartzite is exposed west of the field area. Using Hunt and

Mabey's map (1996), I measured the lower member of the Stirling at approximately 350 m thick. No fossils were observed within the lower member of the Stirling Quartzite. The boundary between the lower member and the middle member is marked by a significant lithologic change of thinly bedded shale layers of the middle member overlying the massive quartzite of the lower member.

Stirling Quartzite (pCs₂) middle shale member

The middle 60 m of the Stirling Quartzite is mainly purplish blue to dusky red, shaly to platy, fine-grained shale interbedded with fine-grained quartzite. Thin layers of brown dolomite are locally present. Ripple marks and mud cracks are present on the partings of the shale layers. At a distance, this member appears platy and bluish red. It is less resistant than the surrounding members and commonly is slope forming.

The middle member of the Stirling Quartzite is strikingly similar to the middle member in the southern Nopah Range; however, colors differ. The middle member in the Nopah Range varies in color from greenish-gray to reddish-brown. In my area, the middle Stirling Quartzite is approximately 60 m thick. I found no fossils. The boundary between the middle member and upper member of the Stirling Quartzite is marked by massive, fine-grained quartzite overlying platy shale.

Stirling Quartzite (pCs₃) upper shale member

The upper 300 m of the Stirling Quartzite is mainly white to gray, but commonly tinted yellow, light red, and orange, fine- to coarse-grained, well-sorted quartzite. It

contains thick beds 30 cm to 1.5 m in thickness and weathers to reddish brown. Well-developed cross-beds are present throughout the member. Some layers contain well-rounded quartzite pebbles. At a distance, it appears as massive brownish-red to orange gray beds. It is highly resistant to erosion and characteristically cliff forming.

The upper member of the Stirling Quartzite is similar to the upper member in the southern Nopah Range. In isolated outcrops, the upper member is difficult to distinguish from the lower quartzite member. In the mapped area, a full section of this member is not observed because it is truncated by faults. It has a minimum thickness of 240 m. I found no fossils. The contact between the upper member of the Stirling Quartzite and the Wood Canyon Formation is marked by alternating shale and quartzite layers of the Wood Canyon Formation that conformably overlie the massive quartzite of the upper Stirling Quartzite.

Wood Canyon (pCs₁) lower shaly member

In the Hanaupah Canyon area, the Wood Canyon Formation can be divided into three members. The lower member consists of thin beds of alternating shale and well-sorted quartzite, and it contains subordinate layers of shaly to sandy dolomite. The shale beds are commonly greenish gray and yellowish brown, varying to shades of orange, and red to reddish brown. The sandstone is fine-grained and generally orange to yellowish brown and weathers dark-brown to an olive-brown. The dolomite weathers orange to yellowish brown. Shale beds constitute approximately 25% of the lower half and most of the upper half of the lower member. Thickness of individual beds ranges from 10 cm to 1

m. At a distance the lower member appears as platy, thin beds of shale, orange to yellowish brown. This member is generally less resistant to erosion than surrounding layers, and therefore is slope forming.

The lower member of the Wood Canyon Formation is similar to the lower member in the southern Nopah Range; there are only slight differences in color. A full section of the lower Wood Canyon Formation member is not present in the mapped area. It has a minimum thickness of 90 m. I found no fossils within the lower member. The boundary between the lower member and middle member of the Wood Canyon Formation is subtle. The lower shaly member gradually changes to the massive quartzite of the middle member.

Wood Canyon (pCs₂) middle red quartzite member

The middle member consists of thick layers of well-sorted quartzite interbedded with platy shale. The quartzite is reddish gray to gray and weathers to red in the lower portion. The upper portion is brownish red to gray and weathers to reddish brown. The quartzite is commonly coarse grained at the base, consisting of gritty, pebbly layers with red jasper pebbles, but becomes progressively finer upward where the upper portion is predominantly fine-grained. The quartzite layers may be up to 2 meters thick. The shaly layers range from grayish red to greenish gray, and become progressively more abundant upward. The quartzite layers are abundantly cross-bedded throughout the member. The basal layers of the middle member contain gritty pebbles of quartz and red jasper. From

a distance, the member appears as red massive layers of quartzite. It is resistant to erosion and commonly cliff forming.

The middle member of the Wood Canyon Formation is very similar to the middle member in the southern Nopah Range and differs only in color. In the Hanaupah Canyon region, the middle member is approximately 210 m in thickness. I found no fossils in the middle member. However, sand-clasts of trilobite fragments and brachiopod shells have been found in the uppermost portion of this member in the southern Nopah Range (Hazzard, 1937). The boundary between the middle and upper member of the Wood Canyon Formation is sharp. The contact is marked by brown dolomite of the upper member, conformably overlying greenish gray shale of the middle member.

Wood Canyon (pCs₃) upper brown dolomite member

The upper member consists of thick layers of dolomite, which are visible in both the southern Nopah Range and north of Resting Springs along the west front of the Resting Springs Range. The dolomite is a dense, dark gray rock with a sandy texture, and is well bedded. Commonly interbedded layers of dark brown, cross-bedded quartzite and greenish gray to reddish layers of shale constitute the upper portion. The weathered surface of the dolomite is a rusty brown to creamy brown color. Subtle cross-beds are present within the dolomite. The upper portion is capped by a pinkish gray shale and sandstone. At a distance, it appears as a dark brown, massive, and moderately resistant layer.

The upper member of the Wood Canyon Formation is similar to the upper member in the southern Nopah Range. However, in the Hanaupah Canyon area, the dolomite layers are not as thick, and the member contains a higher percentage of interbedded shale than do correlative rocks in the southern Nopah Range. In the Hanaupah Canyon area, the upper member is approximately 55 m thick. I saw no fossils in the upper member. The contact between the upper member of the Wood Canyon Formation and the Zabriskie Quartzite is sharp and easily observed from a distance.

Zabriskie (Cz) Quartzite

The Zabriskie Quartzite was originally included in the Wood Canyon Formation. However, due to unique characteristics and widespread deposition, Hazzard (1937) proposed to consider it as a unique formation and named it the Zabriskie Quartzite. This formation consists of thick, massive, fine-grained, crystalline, and well-sorted quartzite. The basal layer of the lower portion is light gray to white, reddish brown weathering massive quartzite. The upper portion is dense, pinkish to light-gray, well-sorted quartzite, which weathers to a distinct salmon-pink to rusty-brown color. The basal layers contain well-sorted quartzite interbedded with sandy shale, while the upper portion contains massive quartzite from 30 cm to 2 m thick. In the basal layers, there are distinct white, vertical, and circular tube-like structures. The tubes are filled with well-cemented white quartzite, which is distinguishable from the surrounding rock. Cross-beds can be seen within the quartzite of the upper portion. At a distance, the Zabriskie Quartzite appears as a massive, resistant layer of distinct, salmon-pink quartzite.

The characteristics of the Zabriskie Quartzite in the Hanaupah Canyon region are also observed in the southern Nopah Range. The tube-like structures found in the lower portion of the Zabriskie Quartzite are believed to be sand-filled burrows like *Scolithus* (Hazzard, 1937). If these burrows are formed by *Scolithus* then the Zabriskie Quartzite is approximately early Cambrian in age. This hypothesis is also confirmed by the presence of trilobite remains in the formations below and above the Zabriskie Quartzite. A full section of the Zabriskie is observed, but non-exposed faults may exist within the Zabriskie. Therefore, it has a minimum thickness of 115 m. The boundary between the Zabriskie Quartzite and the Carrara Formation is easily discernable. The contact is marked by a change from the massive, salmon pink quartzite of the Zabriskie Quartzite to shale and limestone layers of the Carrara Formation.

Carrara Formation (Cc)

Hazzard (1937) included the Carrara Formation in the upper Wood Canyon Formation. However, he did report that it should be considered a separate formation from the Wood Canyon Formation when considering the Zabriskie Quartzite as a new formation. The Carrara Formation consists of interbedded shale and limestone with few beds of platy quartzite. The shale is predominantly greenish gray to light red and light brown, and the thin layers of limestone are a distinct grayish-blue. The limestone ranges from 30 cm up to 1.5 m in thickness, and it contains abundant algal nodules. The platy quartzite layers show fine lamination on the weathered side, and some poorly developed

cross-bedding and ripple marks. At a distance, the Carrara Formation is slope forming and light gray in color.

The Carrara Formation in the Hanaupah Canyon region contains a higher percentage of shale when compared to the formation in the southern Nopah Range. Hazzard (1937) reported that the Carrara Formation is approximately 200 m in thickness. The Carrara Formation in the Hanaupah Canyon region is considerably thinner than that of the Nopah Range. Few unknown fossil fragments were found in limestone layers. Trilobite and brachiopod fragments are observed in the limestone layers in the southern Nopah Range (Hazzard, 1937). The boundary between the Carrara Formation and Bonanza King Formation is sharp and marked by a distinct change in color. The contact is easily discernable by the dark gray to black color of the Bonanza King Formation that conformably rests upon the bluish gray Carrara Formation.

Bonanza King Formation (Cb)

Only the basal section of the Bonanza King Formation is exposed in the Hanaupah Canyon region. Hazzard (1937) describes in detail the entire lithology of the Bonanza King Formation in the southern Nopah Range. The portion of Bonanza King Formation that is exposed consists of thick, crystalline, gray limestone and dolomite beds ranging from 40 cm to 3 m in thickness. At a distance, the Bonanza King Formation is easily recognized by its unique dark gray color and cliff forming characteristics.

The lower section of the Bonanza King Formation in the Hanaupah Canyon region is similar to the lower section of the Bonanza King Formation in the southern

Nopah Range. I saw no fossils in the Bonanza King Formation in my field area.

STRUCTURAL GEOLOGY OF THE HANAUPAH CANYON AREA

Hunt and Mabey (1966) originally mapped a sequence of west-dipping faults that they interpreted as thrust faults that imbricate the stratigraphy described above. I will show that the west-dipping faults have normal slip and that the basal fault is a normal detachment fault, but not that of a metamorphic core complex as described by Hamilton (1988). My interpretation is based on observations of footwall and hanging wall described in the following paragraphs.

The Hanaupah detachment is exposed on the flank of the eastern side of the Panamint Range north of Hanaupah Canyon and south of Death Valley Canyon (Fig. 2b and Plate 1). It marks the contact between Proterozoic basement gneiss and the upper-plate upper Proterozoic and Cambrian rocks. Detailed mapping of the structure within the basement gneiss and the Proterozoic and Cambrian hanging-wall rocks was carried out along the fault from Hanaupah Canyon to Death Valley Canyon (Fig. 2b). The Hanaupah fault is the basal fault in the field area. Extension of the eastern Panamint Range is evident in east-dipping Proterozoic strata that are cut by the Hanaupah Fault, as well as a variety of west-dipping low- to high-angle normal faults and E-W striking faults (Plate 1).

Plate 1 is a geologic map of the mapped area, located north of Hanaupah Canyon and south of Death Valley Canyon. Figures 5a, 5b, and 5c are interpretive cross-sections that are perpendicular to the strikes of the basal Hanaupah detachment and the Proterozoic and Cambrian rocks. Although the cross-sections are perpendicular to the strike of the detachment fault and hanging-wall faults, they may not be parallel to the slip

direction. Therefore, slip on the hanging-wall faults shown in the cross-sections is the minimum amount of slip. Because of two exposed Riedel structures, indicating slip to the west, and W-E striking tear faults, I interpret dip-slip on the faults.

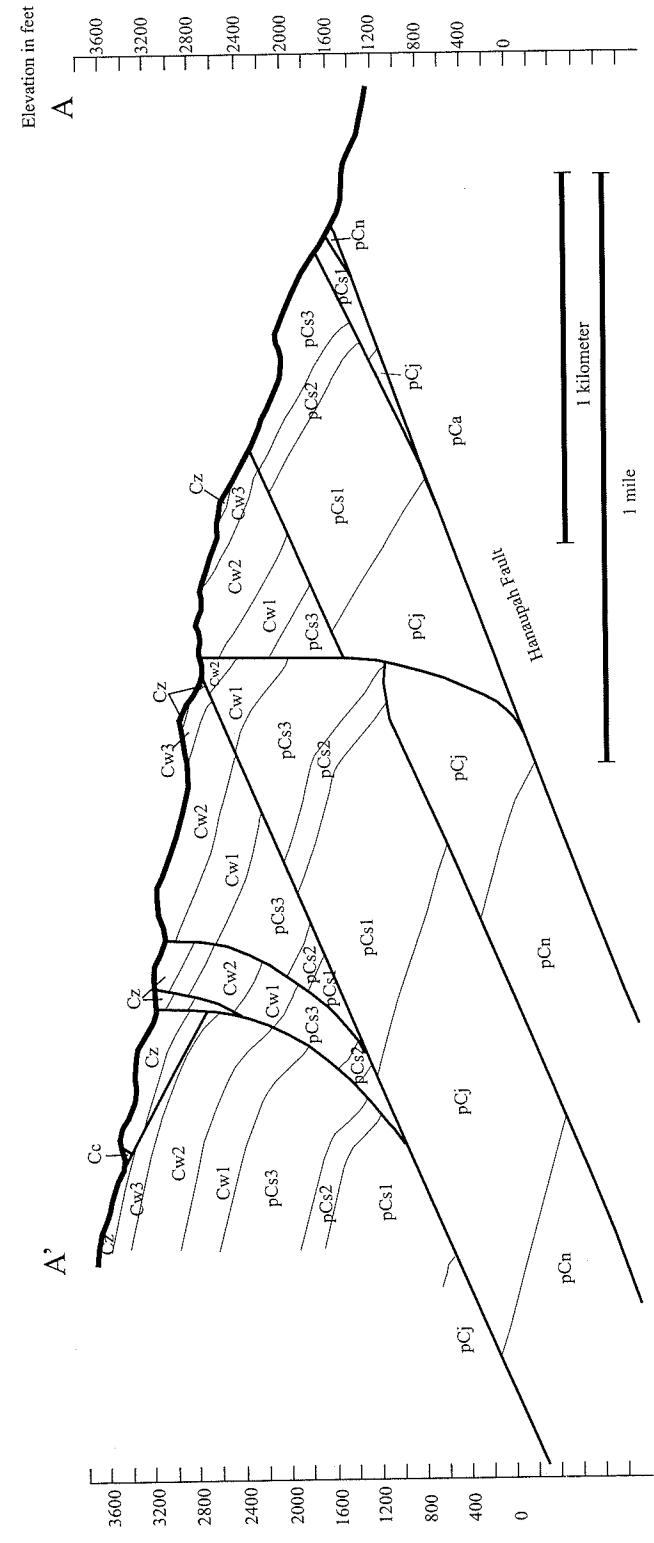


Figure 5a. Cross section A-A' through the southern part of the map area. Abbreviations are: Cc, Carrara; Cz, Zabriskie Quartzite; Cw3, upper Wood Canyon Formation; Cw2, middle Wood Canyon Formation; Cw1, lower Wood Canyon Formation; pCs3, upper Stirling Quartzite; pCs2, middle Stirling Quartzite; pCs1, lower Stirling Quartzite; pCj, Johnnie Formation; pCn, Noonday Dolomite; pCa, augen gneiss basement.

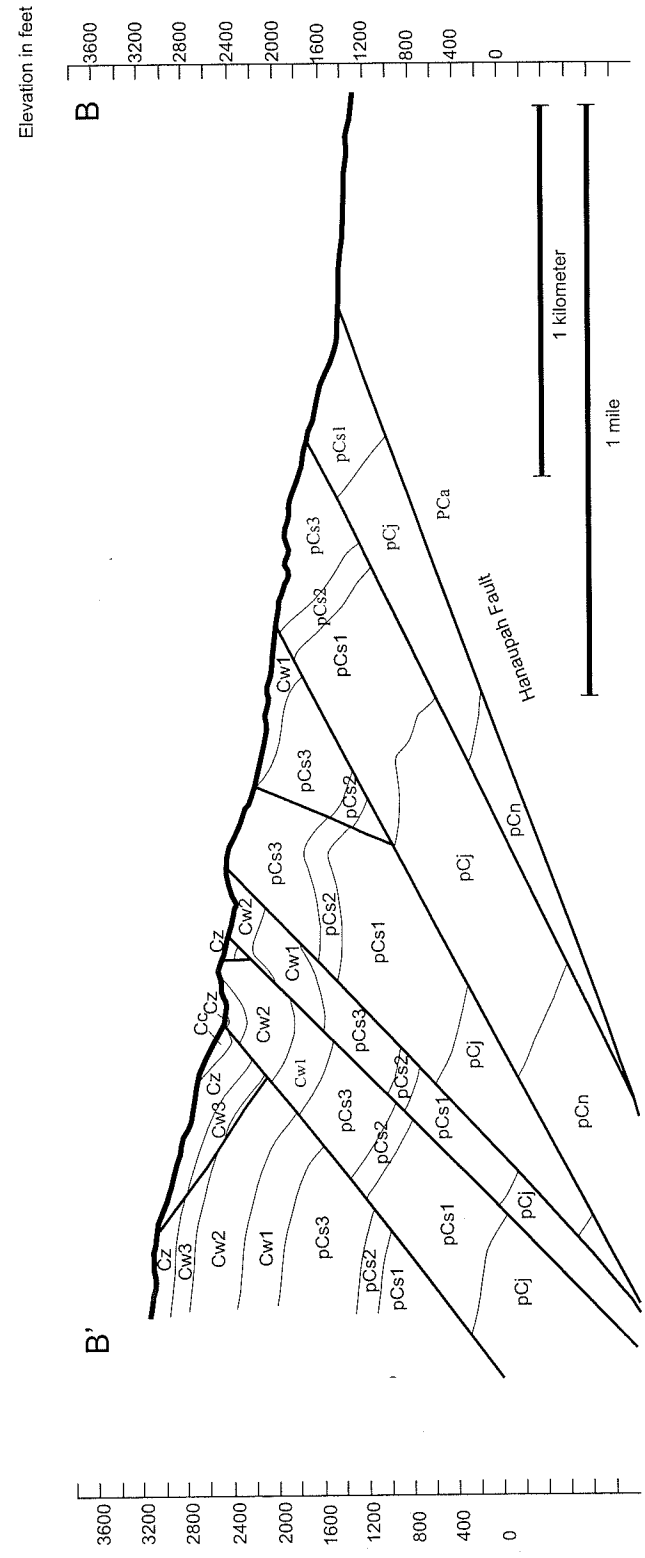


Figure 5b. Cross section B-B' through the middle part of the map area.

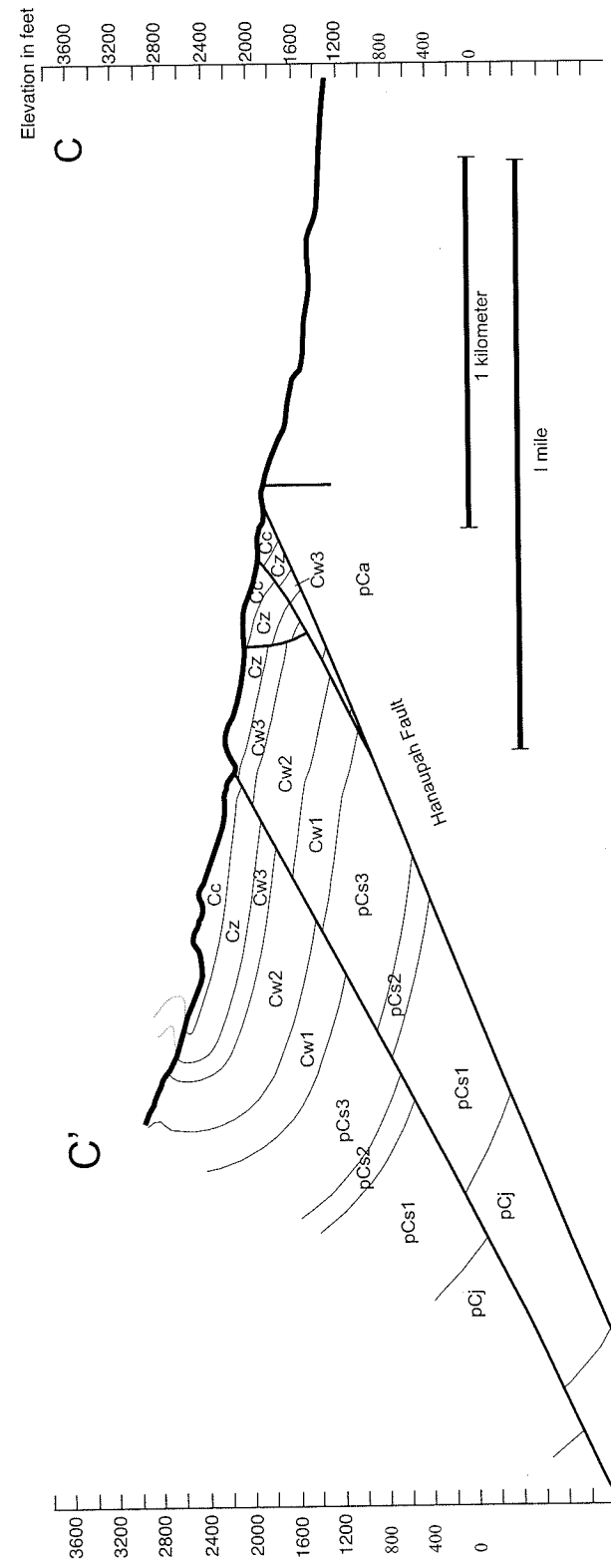


Figure 5c. Cross section C-C' through the northern part of the map area.

FOOTWALL STRUCTURE

The footwall rocks of the Hanaupah detachment (Fig. 4) consist of augen gneiss. The gneissic basement rocks in the Hanaupah Canyon area do not exhibit structural features characteristic of mylonitic basement gneiss in Cordilleran metamorphic core complexes (Davis, 1980; Davis and Coney, 1979; Armstrong, 1982). The basement rocks in the Hanaupah Canyon area have foliation and lineations, but the foliation and lineations vary in orientation, lineations and foliations are not present in the same outcrop. Hamilton (1988) described the augen gneiss as having mylonitic fabrics that increase upward toward the detachment. Upon detailed mapping of the basement rocks, I noted that the feldspathic augen are asymmetrical and show signs of ductile flow (Fig. 6), but sense of slip indicators, such as S-C mylonitic fabrics, mica fish, and rotated porphyroclasts (Simpson and Schmid, 1983; Lister and Snoke, 1984; Passchier, 1994), are absent. Foliation is present in the footwall rocks but the orientation of the foliation varies, and the foliation does not appear to increase upward towards the detachment. The muscovite schist, near the detachment, contains lineations that have a 55° trend and 49° W plunge. Foliation and lineations were not observed in the same outcrop. However, the foliation and lineations that were observed in the basement rocks are overprinted by cataclastic deformation near the detachment. The cataclastic deformation decreases progressively away from the detachment fault. It is possible that the foliation and lineations within the basement rock are pre-extensional features, and the cataclastic deformation is syn-extensional.



Figure 6. Photograph of augen gneiss in the basement rocks of the footwall. The gneiss contains asymmetrical feldspathic augen and exhibits partial ductile texture. View to the southeast.

Figures 7a, b, c, and d show the brittle deformation of the augen gneiss as one approaches the detachment. Approximately 30 m below the detachment, the footwall is composed of coarse-grained, non-mylonitic augen gneiss (Fig. 7a). The augen are composed of potassium feldspar and are slightly asymmetrical. However, the augen cannot be used as kinematic indicators because the axes of elongation exhibit varying orientations. The rock appears to have undergone ductile flow, but it appears not to have been in a tabular zone of high shear strain needed to develop mylonitic fabrics. Approximately 6 m below the detachment, joints develop that cut the feldspar porphyroclasts. These feldspar porphyroclasts are smaller in size (Fig. 7b). The gneiss is slightly brecciated and a bluish tint is apparent.

Approximately 2 meters below the detachment, the footwall rock is highly brecciated (Fig. 7c). In some areas the breccia has a bluish, fine-grained matrix containing clasts of quartz and feldspar. A thin section of the breccia was made and a microprobe study of the matrix was carried out in order to determine what created the bluish tint. The elemental composition of the matrix was determined with BSE and EDS. The matrix was found to be composed of silica, sodium, and aluminum, with microscopic clasts of FeS. The microprobe study did not determine the cause of the bluish appearance. The bluish tint may be the optical effects of an element unresolved by the microprobe, or may be due to the optical properties of particular clay-sized mineral assemblage.

The bluish breccia appears to consist of only footwall material. The breccia is approximately 0.5 m thick and is overlain by fault breccia composed of both footwall and hanging-wall material (Fig 7c and Fig. 7d). The large quartzite clasts within the fault breccia are from the Stirling Quartzite. The matrix is composed of quartzite and material from the footwall and is approximately 0.5 m in thickness. Slightly deformed Stirling Quartzite layers rest upon the fault breccia.

In general, the basement rocks do not contain kinematic indicators or mylonitic fabrics. However, the augen gneiss does exhibit brittle deformation that progressively increases upwards towards the Hanaupah detachment. The Hanaupah detachment strikes approximately 341° and dips 21° W, but the actual fault surface or principal slip plane is nowhere exposed. Proterozoic layers dipping eastward into the basement and cut by the basement rocks mark the Hanaupah detachment fault.

P/S 2 / 5

The bluish breccia appears to consist of only footwall material. The breccia is approximately 0.5 m thick and is overlain by fault breccia composed of both footwall and hanging-wall material (Fig 7c and Fig. 7d). The large quartzite clasts within the fault breccia are from the Stirling Quartzite. The matrix is composed of quartzite and material from the footwall and is approximately 0.5 m in thickness. Slightly deformed Stirling Quartzite layers rest upon the fault breccia.

In general, the basement rocks do not contain kinematic indicators or mylonitic fabrics. However, the augen gneiss does exhibit brittle deformation that progressively increases upwards towards the Hanaupah detachment. The Hanaupah detachment strikes approximately 341° and dips 21° W, but the actual fault surface or principal slip plane is nowhere exposed. Proterozoic layers dipping eastward into the basement and cut by the basement rocks mark the Hanaupah detachment fault.



a



b

Figure 7. Photographs of augen gneiss. **a:** Augen gneiss approximately 30 m below the Hanaupah detachment. The augen are slightly asymmetrical but do not exhibit cataclastic deformation. **b:** The augen gneiss is approximately 6 m below the detachment showing slight cataclastic deformation. **c:** Brecciated augen gneiss 2 m below the detachment. The breccia has a bluish, fine-grained matrix containing clasts of quartz and feldspar. **d:** Breccia approximately 0.5 m below the detachment is overlain by fault breccia composed of basement rocks and clasts of Stirling Quartzite.



Figure 7 (continued).

HANGING-WALL STRUCTURE

The structure of the Proterozoic and early Cambrian rocks in the Hanaupah Canyon area can be divided into Mesozoic contractional structures and Miocene extensional structures. Mesozoic structures occur within the Precambrian and Proterozoic rocks throughout Death Valley and surrounding regions. These structures are primarily east-vergent folds and thrusts of the Sevier orogenic belt (Axen, et al., 1990; Wernicke et al., 1988). Within the Panamint Mountains, NNW-striking anticlines and N-trending, steeply dipping faults are present that developed during Mesozoic time (Labotka et al., 1980; Labotka and Albee, (1990). These Mesozoic structures are observed in the Hanaupah Canyon area. South of Death Valley Canyon, an overturned anticline of Proterozoic and Cambrian rocks is present in the footwall of the Hanaupah detachment. Hunt and Mabey (1966) originally mapped this structure as a thrust fault. North of Hanaupah Canyon, I observed anticlinal and synclinal folds within the hanging wall.

Younger features, such as low-angle faults, truncate these folds and dominate the structure in the hanging-wall. The lower-angle faults are characterized by present day dips of 20 to 26° W, bedding-fault angles of 65 to 80°, brecciated contacts 0.1 to 5 m wide, and dip separations of 200 to 600 meters. These features are well illustrated on Figure 8, which shows a fault contact looking south towards Hanaupah Canyon. The contact is a low-angle normal fault, dipping approximately 20° to the west with a bedding-fault angle of 45°, that juxtaposes lower Stirling Quartzite of the footwall against the middle member of the Wood Canyon Formation of the hanging wall. Figure 9 shows

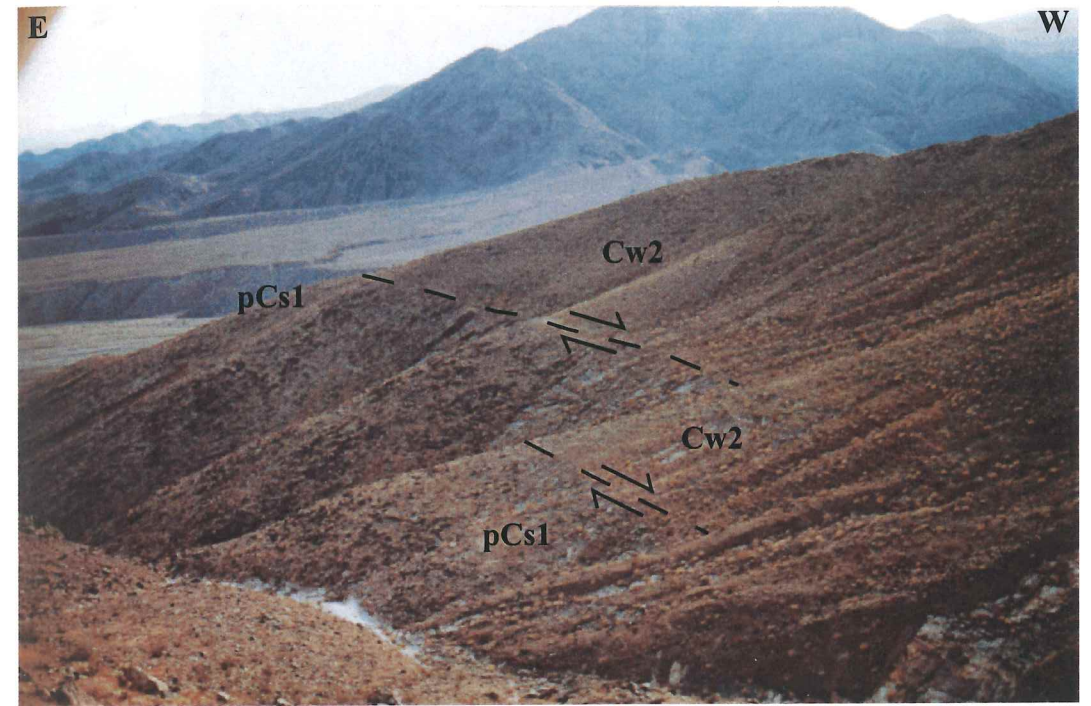


Figure 8. Photograph of a low-angle normal fault in the hanging-wall of the main detachment fault. The low-angle fault is shown as a dashed line, and it juxtaposes lower Stirling Quartzite (pCs1) of the footwall against middle Wood Canyon (Cw2) of the hanging-wall. View to the south.



Figure 9. Photographs of a brecciated contact between upper Stirling quartzite in the hanging-wall and lower Stirling Quartzite in the footwall. The brecciated zone is approximately 1 to 3 m thick. The dashed black line illustrates the low-angle fault and slip direction. Large riedel structures (lime-green color) are present in the hanging-wall. Hammer for scale, view to the south.

an intensely brecciated contact between upper Stirling Quartzite in the hanging wall and lower Stirling Quartzite in the footwall. The low-angle fault dips to the west and contains a brecciated zone, which is 1 to 3 meters thick. The breccia is composed of both upper and lower Stirling Quartzite members. Riedel composite structures (e.g., Cowan and Brandon, 1994) can be seen in the fault gouge and in the hanging-wall layers. The relation of younger-on-older, and the morphology of the breccia suggest normal displacement on this low-angle fault.

Figure 10a is a photograph of a low-angle fault dipping westward at approximately 25° . The fault placed upper Stirling on lower Stirling Quartzite. The beds of upper Stirling are dipping eastward at 30° and are truncated by a sharp fault contact. The brecciated zone is approximately 0.1 to 2 meters thick consisting of upper and lower Stirling. The fault gouge displays Riedel structures, penetrative foliation (P-shears), and a primary slip surface (Figure 10b) (Cowan and Brandon, 1994; Petit, 1987; Hancock, 1985; Rutter et al., 1986). Riedel structures are synthetic normal faults, and they form at an acute angle of about 15° to the fault plane or the boundaries of the shear zone. Penetrative foliation structures are synthetic reverse faults, and they form at a small acute angle of approximately 10° .

The relation of younger on older and the kinematic indicators suggest a top-to-the-west normal displacement. All the low-angle normal faults dip to the west with one exception. In the western region of the Hanaupah Canyon area (Plate 1) is an antithetic, low-angle normal fault. This fault separates lower Zabriskie Quartzite in the footwall from upper Zabriskie Quartzite in the hanging wall. The fault has a dip separation

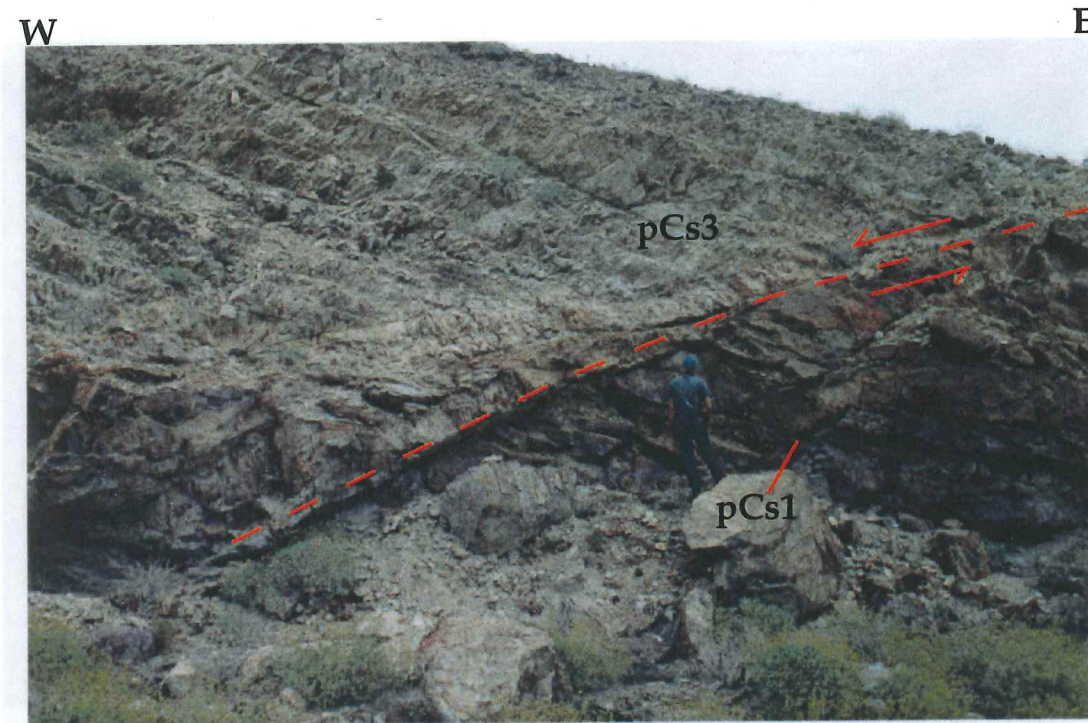


Figure 10a. Photograph of a low-angle normal fault, dipping westward at 25 degrees. The fault is illustrated as a red dashed line, and it displaces upper Stirling Quartzite (pCs3) on lower Stirling Quartzite (pCs1). The breccia zone is .1 to 2 m thick and consists of both lower and upper Stirling Quartzite. The fault gouge displays both Riedel structures and penetrative foliation (Fig. 10b). View to the north.

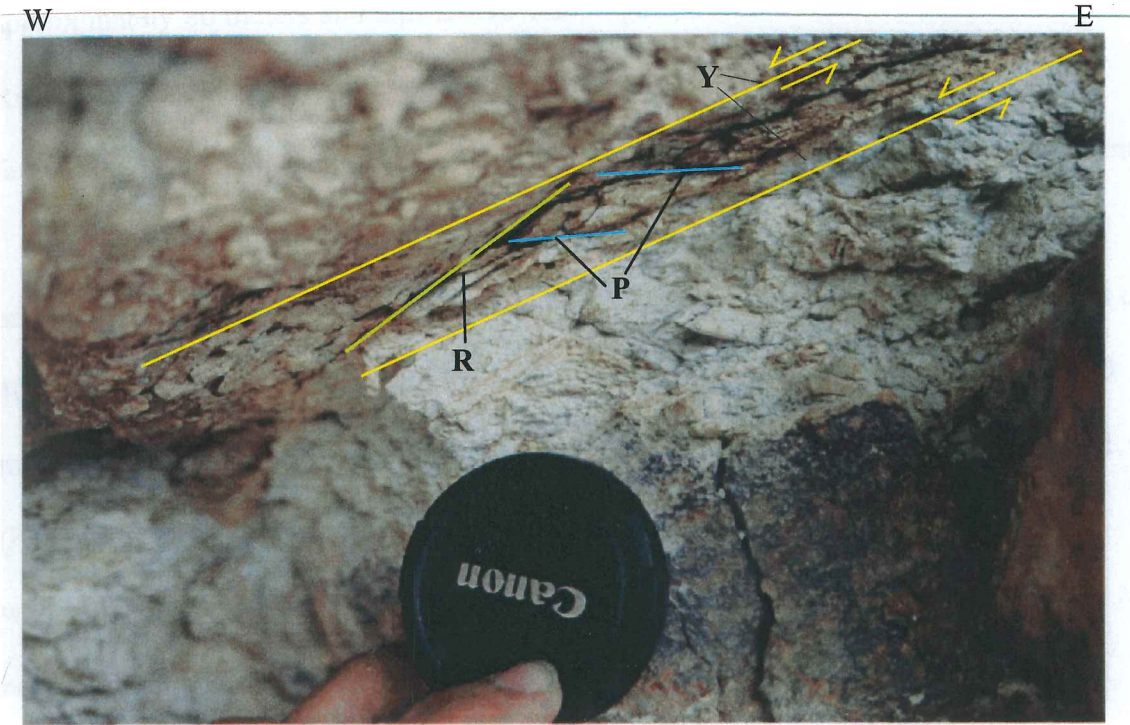


Figure 10b. Photograph of fault gouge from Figure 10a. The gouge displays Riedel structures (R), penetrative foliation or shear fractures (P), and a primary slip surface (Y). The Riedel structures are illustrated with green lines, the penetrative foliation is shown with blue lines, and the primary slip surface is shown with yellow lines. View to the north.

approximately 80 meters and dips 25° E. Although not all the fault contacts exhibit Riedel structures, similar younger-on-older relations are observed on every low-angle fault in the Hanaupah Canyon area. This relationship also suggests normal displacement.

In contrast to the lower angle faults, synthetic and antithetic higher-angle faults are exposed with present day dips of 45 to 81° W and 42 to 85° E, bedding-fault angles of 40 to 60° , sharp, unbrecciated and brecciated contacts, and dip separations of 15 to 260 meters. These structures are present in the southwest region of the field area I mapped (Plate 1), where a high-angle normal fault places upper Wood Canyon in the hanging wall above lower Stirling Quartzite in the footwall. The fault dips 81° to the west, has a bedding-fault angle of 70° , and has a sharp contact. Kinematic indicators that provide sense of slip were not observed in this high-angle fault. However, the relation of younger-on-older rocks suggests that this fault has normal displacement. High-angle, antithetic faults were also observed in the Hanaupah Canyon region. A high-angle normal fault that dips to the east at approximately 50° and has a bedding-fault angle of 45° is exposed in the southwest region of my map (Plate 1). The fault displaces lower Wood Canyon on lower Stirling Quartzite. A breccia zone that varies from a few centimeters to a meter thick marks the contact. This breccia is coarse-grained and composed of the lower Wood Canyon Formation. The younger-on-older relation implies normal displacement. Because younger-on-older relations are seen on all high-angle faults, both synthetic and antithetic, displacement was accommodated through normal faulting. The higher-angle faults truncate lower-angle faults, and in turn are truncated by lower-angle faults.



Figure 11. Photograph of a fault scarp (fault marked in yellow) in the Pleistocene alluvial fans draining into Death Valley. Faults cutting the alluvium are visible from aerial photographs and ASTER satellite images (Fig. 2b). View to the south.

N-S striking, high-angle fault scarps are exposed in the alluvial fans that drain from the Hanaupah Canyon into Death Valley. Figure 11 is a photograph of a fault scarp within the alluvial fans located approximately 1.5 km west of the northern most exposure of basement rocks. The fault scarps display up to 3 meters of slip on these faults. The scarps can be seen from aerial photographs and ASTER satellite images (Fig. 2b). They can be traced to the north of the region I mapped, but die-out to the south.

Subvertical NE-SE to E-W striking faults with dip separations of 30 to 200 meters are the third type of fault exposed in the Hanaupah Canyon area. These faults define contacts that are sharp and unbrecciated. The NE-SW to E-W striking faults appear to truncate N-S striking low-angle faults in the southwest region of Plate 1. However, they are truncated by both N-S striking low-angle and higher-angle normal faults. These relationships suggest that the timing of displacement of the NE-SE to E-W faults is synchronous with low-angle faulting. The E-W to NE-SW faults are not dominant structural features within the hanging wall. They may have developed syntectonically with the low-angle faults as tear faults or transform faults (Gibbs, 1984). If this interpretation is true, the slip direction is parallel to the orientation of these faults.

STRUCTURAL INTERPRETATION

The basement rock in the footwall of the Hanaupah fault has been regarded as mylonitic augen gneiss that records up to tens of kilometers of slip (Hamilton, 1988; Hunt and Mabey, 1966). Upon detailed structural mapping, the basement rocks do not exhibit mylonitic fabrics but rather cataclastic deformation associated with slip. The absence of mylonitic fabrics suggests that a tabular zone of high shear strain did not exist along the detachment zone. The basement rock may be stratigraphically high in the section of the augen gneiss.

Three structural interpretations of the detachment fault can be inferred from the cross-sections in Figures 5a, 5b, and 5c. The first interpretation is that the Hanaupah fault is the sole fault of an extensional duplex: it initially slipped at a higher angle, and the entire duplex has since undergone eastward rotation about an approximately horizontal axis. The second hypothesis is that the Hanaupah fault is a reactivated Mesozoic thrust fault. The third interpretation is that the detachment fault initiated at a low angle and it is listric in nature.

McKenna and Hodges (1990) suggested that the Eastern Panamint fault system is an extensional duplex because of the evidence of sole and roof faults bounding oblique and transfer faults in the Trail Canyon area (McKenna and Hodges, 1990). These attributes conform to Gibb's definition of an extensional duplex (Gibbs, 1984). According to Gibbs (1984), extension is accommodated on listric sole faults. However, as a result of the unloading of the footwall, a second listric fault forms, cutting back towards the undeformed footwall as extension proceeds. This creates a new sole fault,

and displacement on the earlier formed fault ceases to exist. The old sole fault is now a roof fault. The sole and roof faults form bounding surfaces, between which roof-parallel and oblique normal faults extend the rocks within the duplex. The oblique faults do not displace the sole, roof, or roof-parallel faults (Figure 12).

The structurally highest, lower angle fault in the Hanaupah Canyon area corresponds to the Burro Trail Fault, mapped by Hunt and Mabey (1966), and the structurally lowest fault is the Hanaupah detachment. McKenna and Hodges (1990) stated that the Burro Trail fault serves as an upper structural bound for the Eastern Panamint system and the Hanaupah fault is the lowest structural bound. They also suggested that all the faults in the Eastern Panamint fault system, including the Hanaupah fault, initiated at high angles, and the present shallow dips of the faults are due to syn- to postdeformational rotation of the entire duplex.

In the Hanaupah Canyon region, the Hanaupah fault can be considered a sole fault, but the Burro Trail fault cannot be interpreted as a roof fault (as suggested by McKenna and Hodges, (1990)) because several sub-parallel, low-angle normal faults are exposed west of the Burro Trail fault. Also in the Hanaupah Canyon region, the high-angle normal faults or oblique faults offset the roof-parallel faults. These observations contradict the extensional duplex hypothesis proposed by McKenna and Hodges (1990). The Proterozoic and Cambrian strata in the hanging wall are tilted to the east with average dips of 20 to 25°. McKenna and Hodges suggested that the hanging-wall faults were initiated as high-angle faults when the strata were horizontal, and that faults have since been rotated. Two alternative explanations are: 1) the hanging-wall faults may have

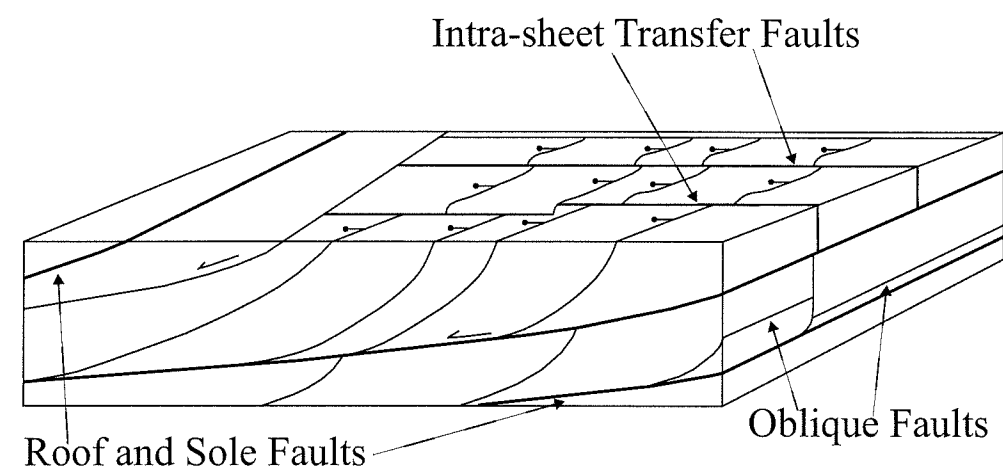


Figure 12. Block model for an extensional duplex, taken from McKenna and Hodges (1990). The subparallel roof and sole faults bound a number of oblique normal faults (black lines with ball symbols). Intrasheet transfer faults separate areas of varying extension on the roof, sole, and parallel faults.

initiated at present day dips (after the strata were rotated), or 2) the section of hanging-wall faults that is exposed today may be the lower portion of listric normal faults and the steeper portions of these listric faults have since been eroded.

The second hypothesis is that the Hanaupah fault is a reactivated Mesozoic thrust. The Panamint Range displays Mesozoic folds and faults oriented NNW that are part of the Cordilleran fold and thrust belt (Snow and Wernicke, 1989; Snow and Wernicke, 2000; Miller, 1987a). However, field observations conflict with this idea. The normal faults trend approximately N-S while the Mesozoic folds and faults trend NNW. Also, the normal faults in the Hanaupah Canyon region cut the fold axes and axial surface of the Mesozoic folds. If the faults were reactivated Mesozoic structures they would not cut the fold axes. Therefore, I propose that the dominant structural deformation seen in the hanging-wall is due to extension on the listric-shaped Hanaupah detachment fault.

I favor the third hypothesis that the geometry and structure of the hanging wall implies rollover folding and crestal collapse. The easternmost fault is the Hanaupah detachment, which is a gentle west-dipping normal fault separating Proterozoic strata from basement gneiss (Fig. 5a, 5b, and 5c). The hanging-wall layers are rotated so that they are at high angles to the detachment. Within 0.25 km of the detachment fault, the Proterozoic strata display an average dip approximately 35° E. Farther west of the Hanaupah fault, the average dip of the Proterozoic bedding slightly decreases. The increasing dip in the Proterozoic bedding is attributed to rollover folding that created an anticlinal geometry in the hanging wall. Rollover folds resulting from slip along the detachment are characteristic of listric faulting (McClay, 1989; Dula, 1991; Braun et al.,

1994). The limit of rotation within the hanging-wall rollover occurs at the point where the detachment fault flattens out (McClay, 1989). Throughout the Hanaupah Canyon region, the hanging-wall rocks dip to the east, which indicates that the Hanaupah detachment fault does not sole out below the area I mapped. The synthetic and antithetic, low- and high-angle faults in the hanging wall are a result of crestal collapse.

Crestal-collapse graben are associated with well-developed rollover anticlines (McClay, 1989; Braun et al., 1994). Analogue models of extensional fault systems do not suggest that faults associated with crestal collapse occur at low angles. Therefore, I suggest that the low-angle faults exposed in the hanging wall are the lower portion of high-angle listric faults. The upper portion of these faults, along with the Phanerozoic sediments, has since been eroded (Fig. 13). I assume that the low- and high-angle normal faults in the hanging wall intersect the Hanaupah fault at depth, and the faults do not offset the Hanaupah fault.

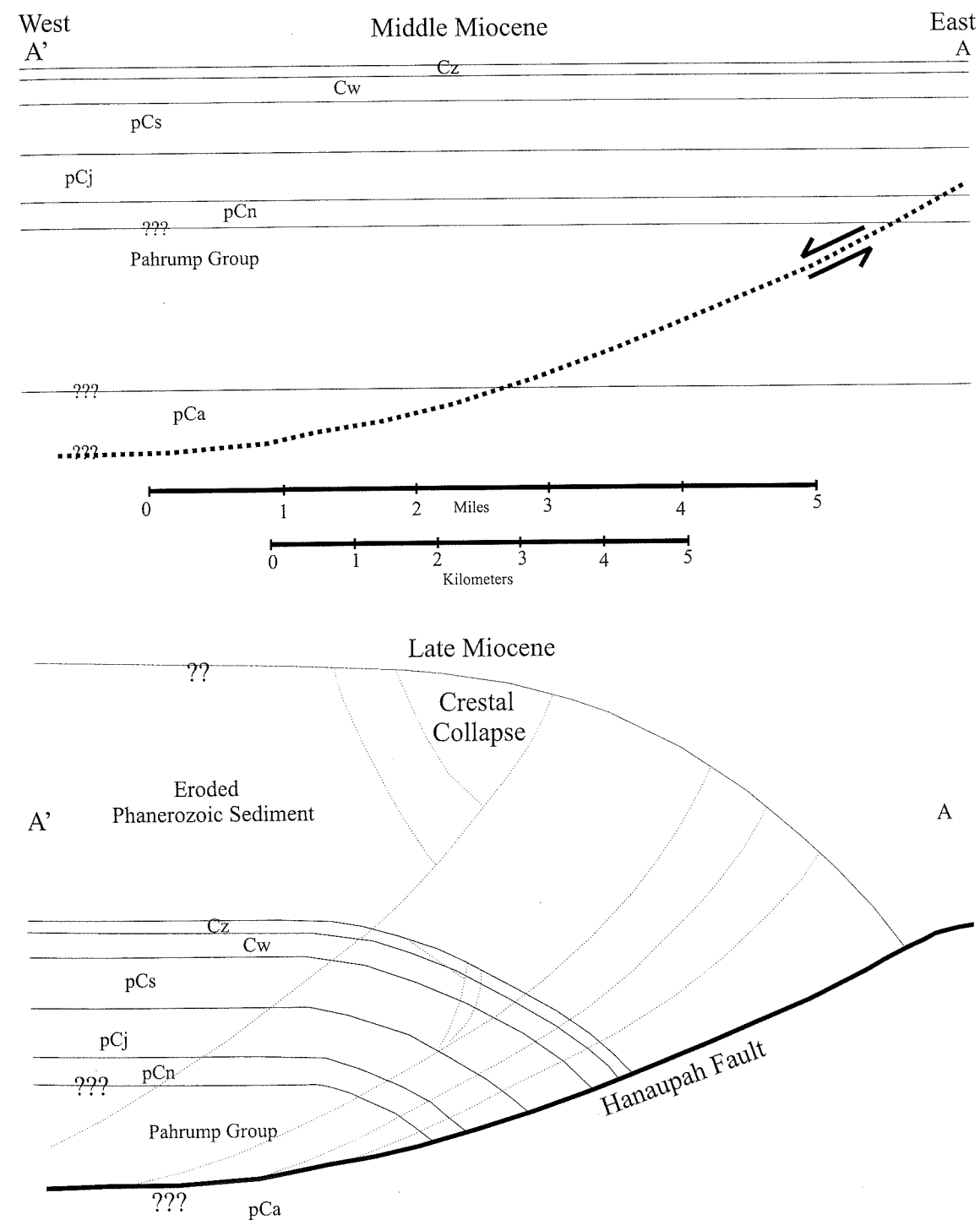


Figure 13. Interpretive cross sections of cross section A-A' from middle to late Miocene. Faults are represented by dark lines, and future faults are represented by dotted lines.

FAULT RECONSTRUCTION

Assuming that the hanging-wall units are continuous and do not change in thickness, deformation of the Hanaupah Canyon area can be restored. Figure 13 shows an interpretation of the structural evolution of the Hanaupah fault as reconstructed along section A-A'. This reconstruction involves rotation of the Proterozoic sedimentary rocks in the hanging wall as the listric faults are restored. Field observations indicate that the Hanaupah detachment, as well as the low-angle and most of the higher-angle faults in the hanging wall, have normal displacement. Motion on the main detachment may have occurred syn-tectonically with slip on the hanging-wall faults.

Restored versions of Section A-A', B-B', and C-C' are shown on figures 14a, 14b, and 14c, respectively. Palinspastic reconstructions were accomplished by drawing multiple cross sections in Corel Draw 7. These cross sections were drawn with various relative ages on the faults and with different fault shapes. Then I restored each cross section by restoring the slip on each fault on separate image layers. However, I could only restore the cross sections by supposing the faults are listric or curved in shape. Therefore, I infer that the Hanaupah fault, as well as the low-angle and most of the higher-angle faults in the hanging wall, are listric. This interpretation contradicts the interpretation of McKenna and Hodges (1990).

McKenna and Hodges's reconstruction (Fig. 5E, p. 371) shows that the Hanaupah fault (Chuckwalla fault) was originally steeply dipping to the west, and present day shallow dips are due to syn- to postdeformational rotation of the Hanaupah fault (1990). In contrast, my reconstruction shows that rotation of the hanging wall is mostly due to

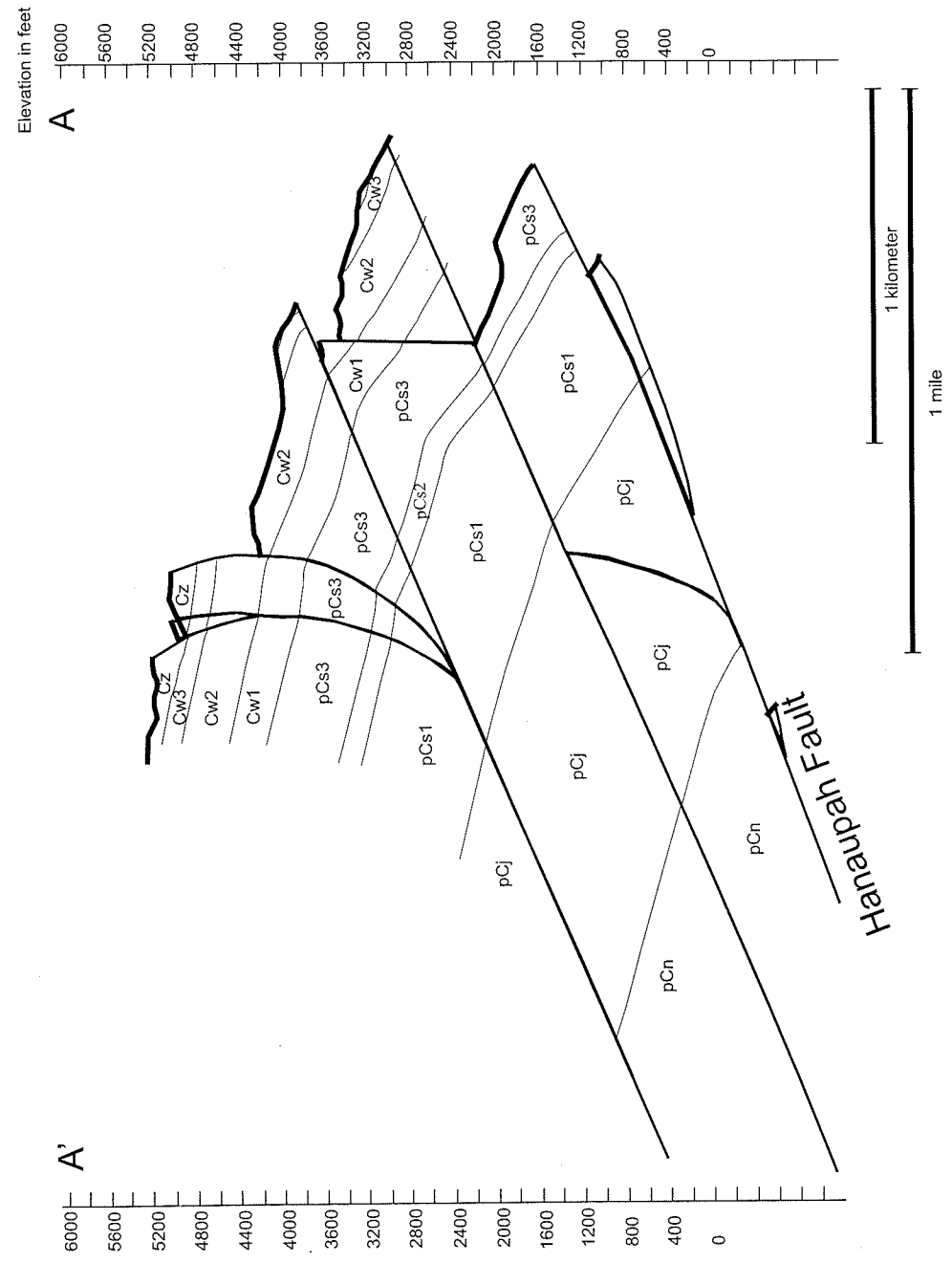


Figure 14a. Restored version of cross section A-A'.

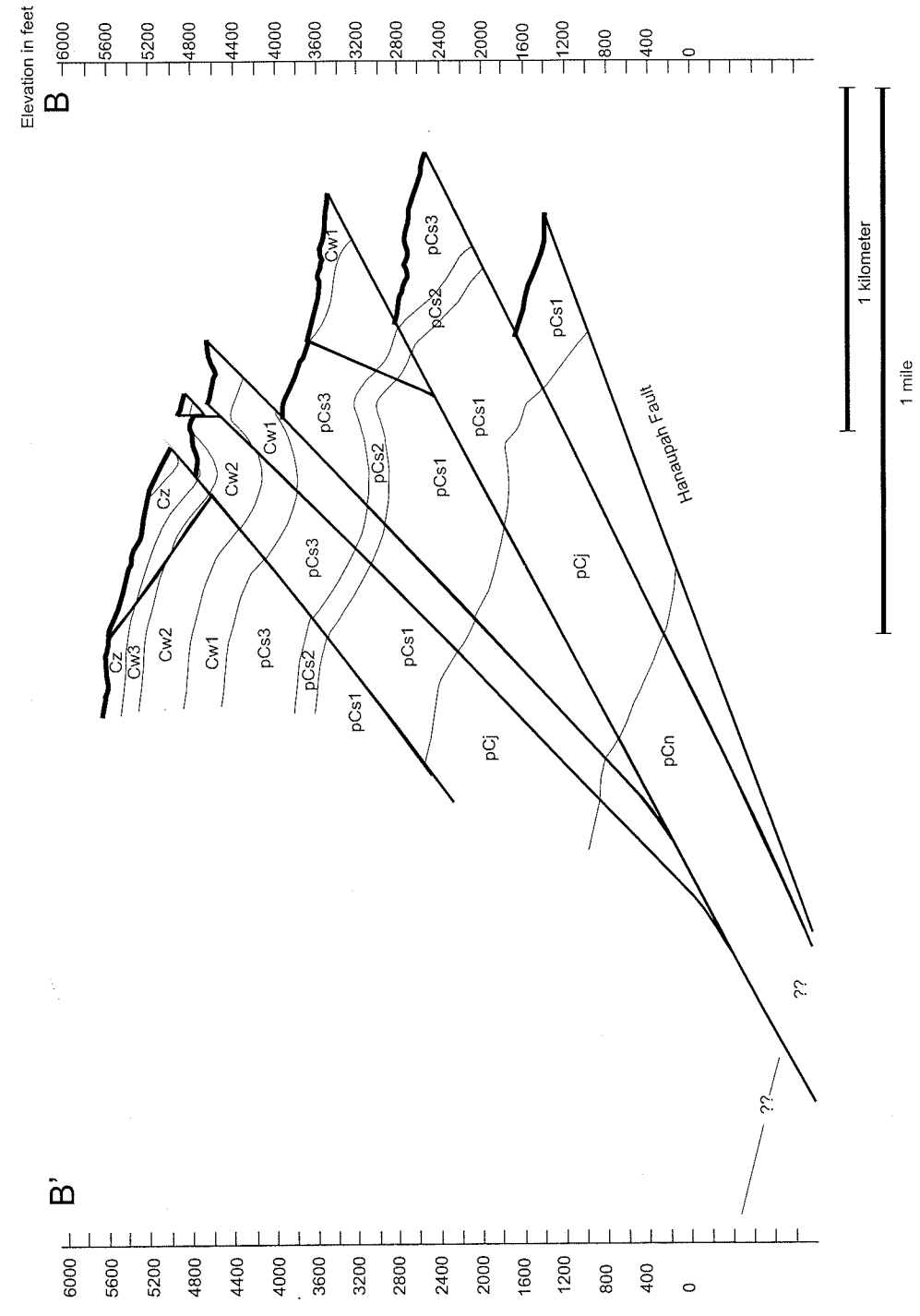


Figure 14b. Restored version of cross section B-B'.

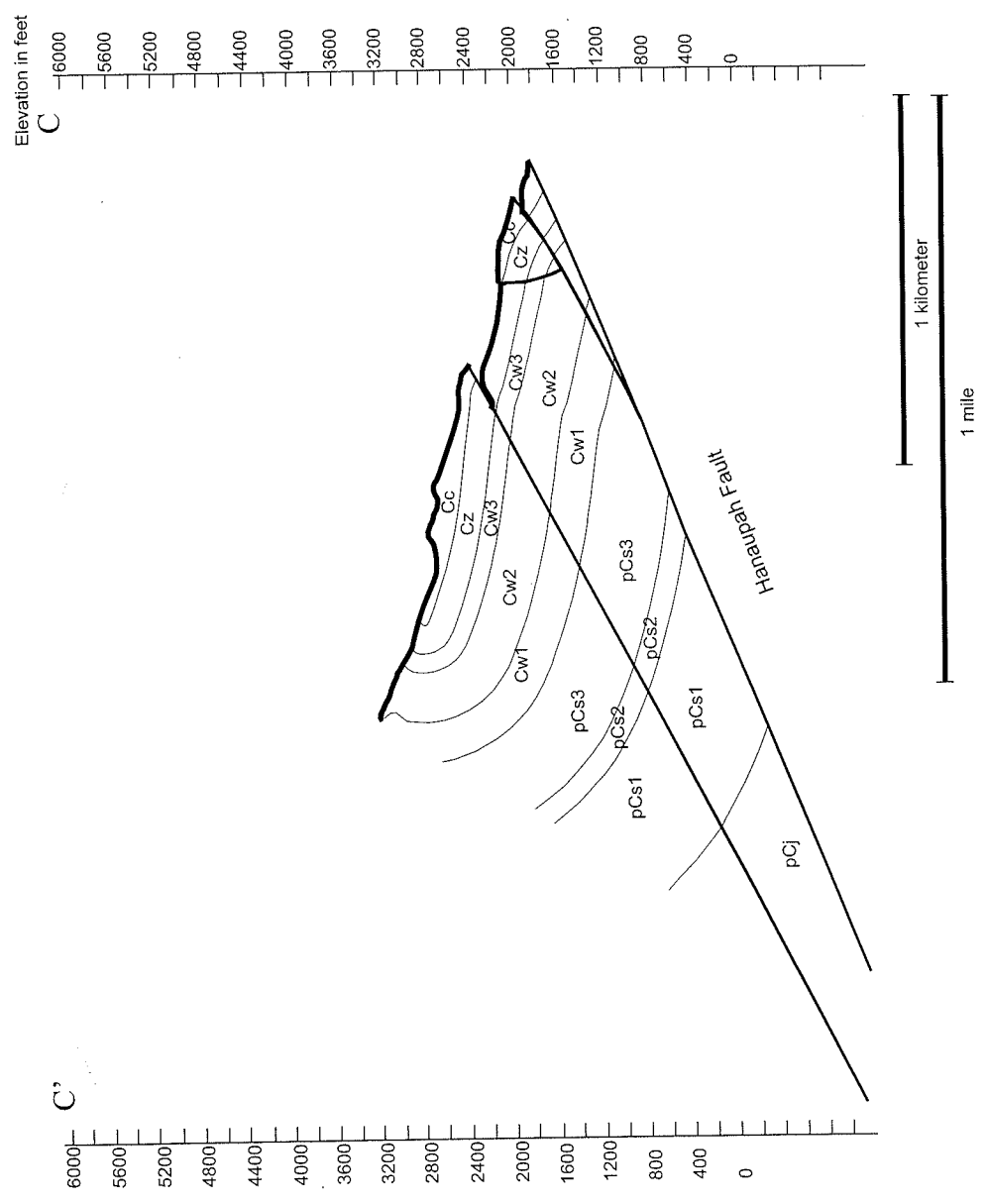


Figure 14c. Restored version of cross section C-C'.

rollover folding due to the listric shape of the Hanaupah fault (Fig. 13). Despite these two conflicting interpretations, my estimates of displacement are similar with McKenna and Hodges's estimates.

Total dip separation within the hanging wall is approximately 1.6 km. Extension within the exposed portion of Proterozoic rocks above the Hanaupah fault is approximately 88 to 100 percent. This is a minimum amount because it assumes that the cross-sections are drawn parallel to the slip-direction. However, these data do not include extension accommodated by the main detachment. The amount of extension would dramatically increase if we include slip on the Hanaupah fault; however, I cannot make an accurate estimate on the displacement of the Hanaupah fault.

In Section A-A', the Hanaupah fault juxtaposes lower Stirling Quartzite with basement augen gneiss. A small sliver of Noonday Dolomite is exposed near the fault. Assuming that the Noonday Dolomite overlies the basement rocks, this sliver suggests that the minimum slip along the Hanaupah fault clearly exceeds 2.2 km (the approximate thickness of Johnnie and Noonday strata). However, according to Wright and Troxel (1967), the Kingston Peak Formation (upper Pahrump Group) is exposed in the upper part of Hanaupah Canyon. In the eastern Panamint Range, the Kingston Peak Formation underlies the Noonday Dolomite, and in the southern Panamint Range the Crystal Spring Formation underlies the Noonday Dolomite (Wright and Troxel, 1967). The Beck Springs Formation does not crop out within the Panamint Mountains, which indicates that either the Beck Springs Formation was not deposited in the area, or that it is not exposed.

Assuming that the Kingston Peak, Beck Springs, and Crystal Springs Formations underlie the Noonday Dolomite and that the upper portion of the basement rock is exposed, a maximum-minimum estimate for displacement on the Hanaupah fault could be approximately 8.0 to 8.4 km. This estimate has an uncertainty of a few hundred meters, reflecting uncertainty about the thickness of each formation within the Pahrump Group. Also, we do not know which section of the basement rocks is exposed in the Hanaupah Canyon area. I make a conservative estimate of slip on the Hanaupah fault by assuming that the upper 10 meters of the Precambrian basement rocks is exposed in the footwall. This estimate assumes that the basement rocks in the Hanaupah Canyon area are at the highest possible stratigraphic level, just below the basal unconformity, prior to extensional faulting.

AGE OF THE HANAUPAH DETACHMENT

Timing of extension on many detachment faults in the Basin and Range Province can be constrained by a variety of isotopic and fission track methods on mylonitic fabrics. Unfortunately, the basement rocks in the Hanaupah Canyon do not contain mylonitic fabrics associated with displacement on the Hanaupah fault. Stern et al., (1966) reported K-Ar ages for biotites from the basement rock of 14 ± 1.5 and 11 ± 1 Ma (recalculated by McKenna and Hodges (1990) using decay constraints of Steiger and Jäger, 1977). However, the basement rocks are cut by a sequence of sub-vertical dikes that do not intrude the hanging-wall rocks. Therefore, these ages probably reflect cooling of the gneiss after the intrusion of these dikes. North of my field area, McKenna and Hodges note that volcanic rocks of the Trail Canyon Volcanic Sequence are exposed. Because the units of the Trail Canyon Volcanic Sequence are cut and rotated by Eastern Panamint System, McKenna and Hodges (1990) suggested that the timing of slip is late Miocene and younger in age.

DISCUSSION AND CONCLUSIONS

The Hanaupah fault developed in late Miocene time (McKenna and Hodges, 1990; Hodges et al., 1990), and felsic dikes intruding the footwall suggest that the slip is no older than 15 ± 1.5 Ma. My structural reconstructions indicate that the Hanaupah fault is listric in nature, which created rollover folding in the hanging wall. Kinematic indicators show that the high- and low-angle faults within the hanging wall have normal displacement and are a result of crestal collapse (McClay, 1989; Braun et al., 1994). Cross-sections and palinspastic reconstructions suggest that the low- and high-angle faults in the hanging wall are listric. Other low-angle normal faults exist in the hanging wall west of the Hanaupah Canyon area and are locally offset by higher-angle normal faults (Hunt and Mabey, 1966). The present day structure of the eastern Panamint Range in the Hanaupah Canyon region is the consequence of rollover folding due to slip on the Hanaupah fault. These observations contradict McKenna and Hodges's idea of a rotated extensional duplex, and my interpretation of rollover folding disagrees with McKenna and Hodges's Figure 5E (1990).

The Hanaupah fault has a stratigraphic displacement exceeding 2.2 km or an upper-minimum value of 8.0 to 8.4 km if in this area the Noonday Dolomite overlay the entire section of the Pahrump Group. Hanging-wall faults generally dip to the west at approximately 20 to 26°. The hanging wall has undergone 88 to 100 percent extension. These are conservative estimates because they do not include slip on the Hanaupah fault, and it is not clear whether the uppermost basement rocks are exposed in the footwall of the Hanaupah fault. This agrees with the displacement estimates calculated by McKenna

and Hodges on the Eastern Panamint fault system (1990). However, evidence from the footwall indicates that the basement is neither mylonitic nor a metamorphic core complex. I cannot make an accurate estimate of the maximum displacement on the fault, because it is not clear which stratigraphic portion of the basement rock is exposed, whether the Noonday Dolomite overlay the entire section of the Pahrump Group, and what the direction of slip is on the Hanaupah fault.

The basement rocks in the footwall of the Hanaupah fault are composed of augen gneiss but do not display any mylonitic fabrics that are associated with displacement on the Hanaupah fault. The metamorphic fabrics, lineations, and foliations displayed in the footwall may have been pre-extensional features. The footwall does not exhibit the structures that are characteristic of a metamorphic complex (Davis and Coney, 1979; Davis, 1980; Coney, 1980). However, cataclastic deformation in the footwall increases towards the Hanaupah fault, and I infer that the cataclastic deformation is related to displacement on the fault.

The central Panamint Mountains do contain lower greenschist to amphibolite facies metamorphic rocks that make up the Panamint metamorphic core complex (McKenna et al., 1990). Hodges et al. (1990) suggested that unroofing of the Panamint metamorphic core complex was accommodated by movement on the Harrisburg and Emigrant faults, with several kilometers accommodated by the Eastern Panamint fault system. Within the Eastern Panamint fault system, the Hanaupah fault accommodated most of the displacement. The present day position of the Panamint Mountains may be the consequence of slip on both the Amargosa system and the Hanaupah fault, with the

Amargosa system accommodating most of the displacement and the Hanaupah fault accommodating only several kilometers of slip.

My field research in Hanaupah Canyon did not yield evidence bearing on the question of whether or not the Panamint Mountains have undergone large or small amounts of NW displacement (Stewart, 1983; Cemen et al., 1985; Wernicke et al., 1988; Hamilton, 1988; Wright et al., 1991; Topping, 1993; Serpa and Pavlis, 1996; Petronis et al., 2000; Schauble, E, 2002; Miller, personal commun.). Most of the NW displacement of the Panamint Range has been accommodated on other faults within the Death Valley region. The presence of fault scarps in the alluvial fans, northeast of my area, indicates that extension of the Death Valley region is relatively recent, and the Death Valley region may be undergoing extension today.

References Cited

- Armstrong, R.L., 1982, Cordilleran metamorphic core complexes; From Arizona to southern Canada: Annual review of Earth and Planetary Science, v. 10, p. 129-154.
- Asmerom, Y., Snow, J.K., Holm, D.K., Jacobson, S.B., Wernicke, B.P., and Lux, D.R., 1990, Rapid uplift and crustal growth in extensional environments: An isotopic study from the Death Valley region, California: *Geology*, v. 18, p. 223-226.
- Axen, G.J., Wernicke, B.P., Skelly, M.F., and Taylor, W.J., 1990, Mesozoic and Cenozoic tectonics of the Sevier thrust belt in the Virgin River Valley area, southern Nevada: *GSA Memoir* 176, p. 123-153.
- Brady, R.J., Wernicke, B.P., and Niemi, N.A., 2000, Reconstruction of the Basin and Range extension and westward motion of the Sierra Nevada Block, *in* Lageson D.R., ed., *Great Basin and Sierra Nevada: Geological Society of America, Field Guide* 2, p. 75-96.
- Braun, J., Batt, G.E., Scott, D.L., McQueen, H., and Beasley, A.R., 1994, A simple kinematic model for crustal deformation along two- and three-dimensional listric normal faults derived from scaled laboratory experiments: *Journal of Structural Geology*, v. 16, no. 10, p. 1477-1490.
- Burchfiel, B.C., and Stewart, J.H., 1966, "Pull-apart" origin of the central segment of Death Valley, California: *Geological Society of America Bulletin*, v. 77, p. 439-442.
- Cemen, I., Wright, L.A., Drake, R.E., Johnson, F.C., 1985, Cenozoic sedimentation and sequence of deformational events at the southeastern end of the Furnace Creek strike-slip fault zone, Death Valley region, California, *in* Biddle, K.T., and Christie-Blick, N., eds., *Strike-slip deformation, basin formation, and sedimentation: Society of Economic Paleontologists and Mineralogists Special Publication* 37, p. 127-141.
- Coney, P.J., 1980, Cordilleran metamorphic core complexes: An overview: *GSA Memoir* 153, p. 7-31.
- Cowan, D.S., and Brandon, M.T., 1994, A symmetry based method for kinematic analysis of large-slip brittle fault zones: *American Journal of Science*, v. 294, p. 257-306.

- Davis, G.H., 1980, Structural characteristics of metamorphic core complexes, southern Arizona, *in* Cordilleran metamorphic core complexes: GSA Memoir 153, p. 35-77.
- Davis, G.H., and Coney, P.J., 1979, Geologic development of the Cordilleran metamorphic core complexes: *Geology*, v. 7, p. 120-124.
- Dula, W.F., 1991, Geometric models of listric normal faults and rollover folds: *American Association of Petroleum Geologists*, v. 75, p. 1609-1625.
- Eaton, G.P., 1982, The Basin and Range Province: Origin and tectonic significance: *Annual Review of Earth and Planetary Sciences*, v. 10, p. 409-440.
- Gibbs, A.D., 1984, Structural evolution of extensional basin margins: *Journal of the Geological Society of London*, v. 141, p. 609-620.
- Hamilton, W.B., 1988, Detachment faulting in the Death Valley Region, California and Nevada: *U. S. Geological Survey Bulletin* 1790, p. 51-85.
- Hancock, P.L., 1985, Brittle microtectonics: Principles and practice: *Journal of Structural Geology*, v. 7, nos. 3/4, p. 437-457.
- Haugerud, R., and Greenberg, H.M., 1997, Recipes for Digital Cartography: Cooking with DEMs: Digital Mapping Techniques, Workshop Proceedings U.S. Geological Survey Open-File Report 98-487.
- Hazard, J.C., 1937, Paleozoic section in the Nopah and Resting Springs Mountains, Inyo County, California: *California Journal of Mines and Geology*, 33; 4, p. 270-339.
- Hodges, K.V., McKenna, L.W., and Harding, M.B., 1990, Structural unroofing of the central Panamint Mountains, Death Valley Region, southeastern California: GSA Memoir 176, p. 377-389.
- Hoisch, T.D., and Simpson, C., 1993, Rise and tilt of metamorphic rocks in the lower plate of a detachment fault in the Funeral Mountains, Death Valley, California: *Journal of Geophysical Research*, v. 98, p. 6805-6827.
- Holm, D.K., and Wernicke, B., 1990, Black Mountains crustal section, Death Valley extended terrain, California: *Geology*, v. 18, p. 520-523.
- Hunt, C.B., and Mabey, D.R., 1966, Stratigraphy and structure, Death Valley, California: U.S. Geological Survey Professional Paper 494-A, 165 p.

- Labotka, T.C., and Albee, A.L., 1990, Uplift and exposure of the Panamint metamorphic core complex, California, *in* Wernicke, B.P., ed., Basin and Range extensional tectonics near the latitude of Las Vegas, Nevada: GSA Memoir 176, p. 345-362.
- Labotka, T.C., Albee, A.L., Lanphere, M.A., and McDowell, S.D., 1980, Stratigraphy, structure, and metamorphism in the central Panamint Mountains (Telescope Peak Quadrangle), Death Valley area, California: Summary: GSA Bulletin, Part I, v. 91, p. 125-129.
- Lister, G.S., and Snoke, A.W., 1984, S-C mylonites: *Journal of Structural Geology*, v. 6, p. 617-638.
- McClay, K.R., 1989, Physical models of structural styles during extension, *in* Tankard, A.J. and Balkwill, H.R., ed., Extensional tectonics and stratigraphy of the North Atlantic margins: Mem. Am. Ass. Petrol. Geol., v. 46, p. 95-110.
- McKenna, L.W., and Hodges, K.V., 1990, Constraints on the kinematics and timing of late-Miocene-Recent extension between the Panamint and Black Mountains, southeastern California: GSA Memoir 176, p. 363-376.
- McKenna, L.W., Hodges, K.V., and Harding, M.B., 1990, Structural unroofing of the central Panamint Mountains, Death Valley region, southeastern California: GSA Memoir 176, p. 377-390.
- Miller, J., 1987a, Tectonic evolution of the Southern Panamint Range, Inyo and San Bernardino Counties: *California Geology*, p. 212-222.
- Miller, J., 1987b, Paleotectonic and stratigraphic implication of the Kingston Peak-Noonday contact in the Panamint Range, Eastern California: *Journal of Geology*, v. 95, p. 75-85.
- Noble, L.F., 1941, Structural features of the Virgin Spring area, Death Valley, California: *GSA Bulletin*, v. 52, p. 941-1000.
- Passchier, C.W., 1994, Mixing in flow perturbations: a model for development of mantled porphyroclasts in mylonites: *Journal of Structural Geology*, v. 8, p. 831-843.
- Petit, J.P., 1987, Criteria for the sense of movement on fault surfaces in brittle rocks: *Journal of Structural Geology*, v. 9, nos. 5/6, p. 597-608.
- Petronis, M.S., Geissman, J.W., M.S., Holm, D.K., Wernicke, B.P., and Schauble, E., 2002, Assessing vertical axis rotations in large-magnitude extensional settings: A

- transect across the Death Valley extended terrane, California: *J. of Geophysical Research*, v. 107, NO. B1, EMP, p. 4-1 to 4-21.
- Rutter, E.H., Maddock, R.H., Hall, S.H., and White, S.H., 1986, Comparative microstructures of natural and experimentally produced clay-bearing fault gouges: *Pure and Applied Geophysics*, v. 124; nos., 1/2, p. 3-30.
- Serpa, L., and Pavlis, T.L., 1996, Three-dimensional model of the late Cenozoic history of the Death Valley region, southeastern California: *Tectonics*, v. 15, p.1113-1128.
- Simpson, C., and Schmid, S.M., 1983, An evaluation of criteria to deduce the sense of movement in sheared rocks: *GSA Bulletin*, v. 94, p. 1281-1288.
- Snow, J.K., and Wernicke, B.P., 1989, Uniqueness of geological correlations: An example from the Death Valley extended terrain: *GSA Bulletin*, v. 101, p. 1351-1362.
- Snow, J.K., and Wernicke, B.P., 2000, Cenozoic tectonism in the central Basin and Range: Magnitude, rate, and distribution of upper crustal strain: *American Journal of Science*, v. 300, p. 659-719.
- Steiger, R.H., and Jäger, E., compilers, 1977, Subcommittee on Geochronology; Convention on the use of decay constants in geo and cosmochronology: *Earth and Planetary Science Letters*, v. 36, p. 97-107.
- Stewart, J.H., 1978, Basin and Range structures in western North America: a review, *in* Smith, R.B., and Eaton, G.L., eds., *Cenozoic Tectonics and Regional Geophysics of the Western Cordillera: Memoir GSA*, v. 152, p. 1-31.
- Stewart, J.H., 1983, Extensional tectonics in the Death Valley area, California: Transport of the Panamint Range structural block 80 km northwest: *Geology*, v. 11, p. 153-157.
- Topping, D.J., 1993, Paleogeographic reconstruction of the Death Valley extended region: Evidence from Miocene large rock-avalanche deposits in the Amargosa Chaos Basin, California: *GSA Bulletin*, v. 105, p. 1190-1213.
- Wernicke, B.P., Axen, G.J., and Snow, J.K., 1988, Basin and Range extensional tectonics at the latitude of Las Vegas, Nevada: *GSA Bulletin*, v. 100, p. 1738-1757.
- Wright, L.A., Thomson, R.A., Troxel, B.W., Pavlis, T.L., DeWitt, E.H., Otton, J.K., Ellis, M.A., Miller, M.G., and Serpa, L.F., 1991, Cenozoic magmatic and tectonic

evolution of the east-central Death Valley region, California, *in* Walawender, M.J., and Hanan, B.B., eds., Geological excursions in southern California and Mexico: Annual Meeting, Geological Society of America, San Diego, California, October 21-24, Guidebook, p.93-127.

Wright, L.A., and Troxel, B.W., 1967, Limitation on right-lateral, strike-slip displacement, Death Valley and Furnace Creek fault zones, California: Geological Society of America Bulletin, v. 78, p. 933-958.

Wright, L.A., and Troxel, B.W., 1973, Shallow-fault interpretation of Basin and Range structure, southwestern Great Basin, *in* DeJong, K.A., and Scholten, R., eds., Gravity and Tectonics: New York, John Wiley & Sons, p. 397-407.

Wright, L.A., Otton, J.K., and Troxel, B.W., 1974, Turtleback surfaces of Death Valley viewed as phenomena of extensional tectonics: *Geology*, v. 2, p. 53-54.

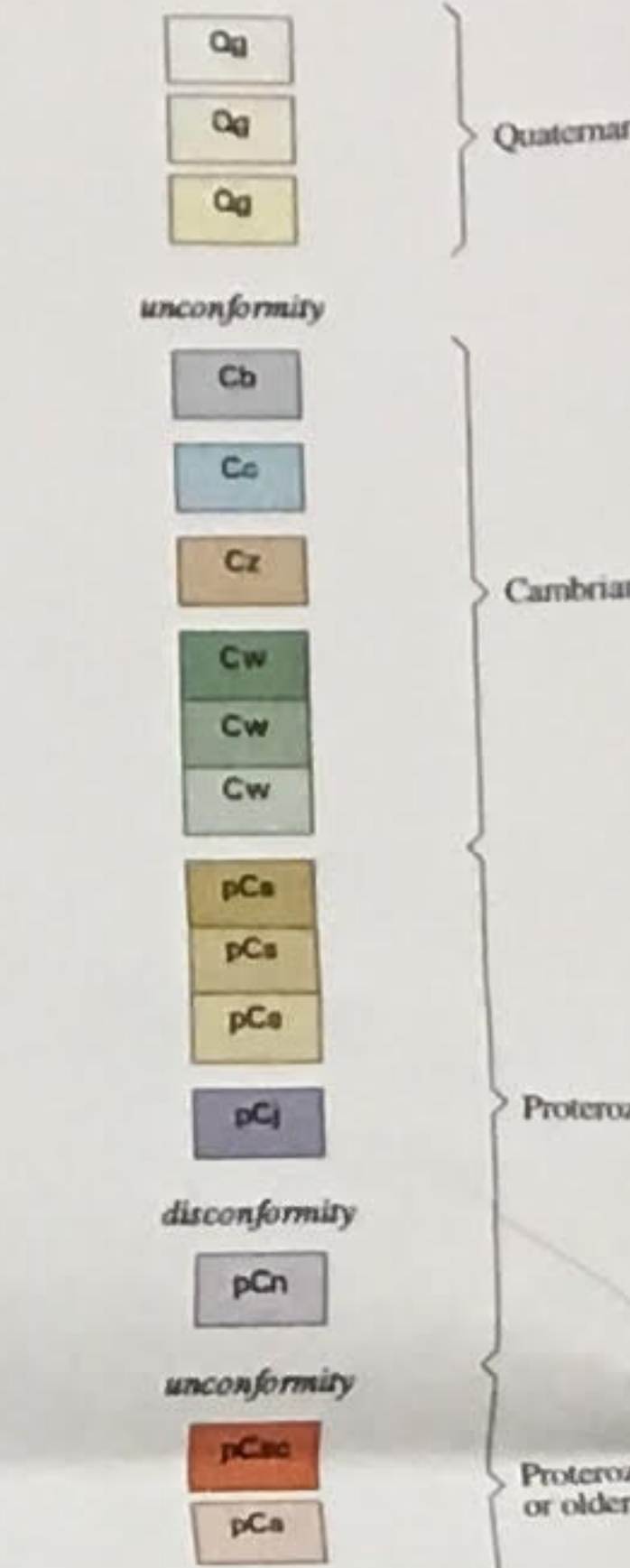
21 371441 2905
TH
8/02 31364-159 NLE



The Nature and Geometry of the Hanaupah fault, Death Valley, California



CORRELATION OF MAP UNITS



Unit Descriptions

Unconsolidated deposits

Qg3 Loose gravel and sand in recent washes. No desert varnish or weathering rinds except in the vicinity of older deposits, in which older gravels are reworked into the wash.

Qq2 Younger of the upper Pleistocene fan gravels. Mostly consists of pebbles to cobble-sized gravel. Stones are strongly varnished, but they lack weathering rinds. Typically found as fans within present washes and faulted in some areas. Surfaces protected from floods exhibits well-developed desert pavement.

Qq1 Older of the upper Pleistocene fan gravels. Boundary deposits in old fans. Fans form distinct units but are typically dissected. Commonly tilted as well as faulted. Distinct weathering rinds exist on boulders and cobbles. Some desert varnish, but the varnish is less distinct than in younger gravels. Includes beds of ash in Six Spring Canyon.

Quaternary

Cambrian

Cb Bonanza King Formation. Thick, crystalline, gray limestone and dolomite beds ranging from 40 cm to 3 m in thickness. At a distance, the Bonanza King Formation is easily recognized by its unique dark gray color and cliff-forming characteristics.

Cc Carrara Formation. Interbedded shale and limestone with some layers of platy quartzite. Shale is predominantly greenish gray to light red and light brown. The thin layers of limestone are a distinct grayish-blue.

Cz Zabriskie Quartzite. Quartzite, containing interbeds of sandy shale in lower portion and massive quartzite sandstone in the upper portion. The upper portion is dense, pinkish to light-gray quartzite, which weathers to a distinct salmon-pink to rusty-brown in color. The basal layer of the lower portion is light gray to white, reddish brown weathering massive quartzite. In basal layers, distinct white, vertical, circular, tube-like structures exist. The tubes filled with well-cemented white quartzite, which is distinguishable from the surrounding rock. At a distance, the Zabriskie appears as a massive, highly resistant layer of distinct, salmon-pink quartzite.

Proterozoic

Proterozoic or older

Wood Canyon Formation

Cw3 Upper brown dolomite member. Dolomite forms most of the member. It is dense, dark gray, crystalline to fine-grained rock, which weathers to dirty brownish gray, forms lower portion. Commonly interbedded with layers of dark brown, cross-bedded quartzite and greenish gray to reddish layers of shale in the upper portion. At a distance, it appears as a massive, moderately resistant layer of dark brownish dolomite capped by a pinkish gray shale and sandstone.

Cw2 Middle red quartzite member. Quartzite, containing interbedded shale layers that become more abundant in upper portion. This member is commonly coarse-grained at the base consisting of gritty, pebbly layers with red jasper pebbles but becomes progressively finer upward where the upper portion is predominantly fine-grained. Quartzite in lower half is generally pale, reddish gray to gray, which weathers to red, abundantly cross-bedded, and interbedded with layers of grayish red shale. The upper half is fine-grained, brownish red to gray, which weathers to reddish brown, commonly cross-bedded and interbedded with layers of greenish gray shale. The upper most portion contains abundant greenish gray shale with light brown to greenish gray, fine-grained quartz sandstone. At a distance, it appears as massive, red quartz sandstone layers. This member is highly resistant to erosion and is generally a cliff former.

Cw1 Lower shaly member. Shale and quartzite, thin beds of alternating shale and sandstone and containing subordinate layers of sandy dolomite. Shale beds comprise approximately 25% of the lower half and most of the upper half. These shale beds are commonly greenish gray, yellowish-brown to shades of orange, red to reddish brown. The sandstone is fine-grained and generally orange to yellowish brown. Dolomite is fine- to medium-grained and generally brownish gray, which weathers orange to yellowish brown. At a distance, it appears platy, thin beds of shale, orange to yellowish brown. This member is generally less resistant to erosion than bounding formations.

Stirling Quartzite

pCs3 Upper quartzite member. Quartzite, fine- to coarse-grained, white to gray, but commonly tinted yellow, light red, orange, which weathers to reddish brown. Cross-bedding and ripple marks common throughout the member. Locally contains thin lenses well-sorted quartzite pebbles. In isolated outcrops, this member is difficult to distinguish from the lower quartzite member. At a distance, it appears massive, brownish red, orange to gray. It is highly resistant to erosion and generally a cliff former.

pCa2 Middle shale member. Shale and fine-grained, platy quartzite and mostly purplish blue to dusky red. Thin layers of brown dolomite are present. Ripple marks and mudcracks are present on many of the parting surfaces of the shaly sandstone. In the upper portion, platy sandstone layers containing lenses of flat shale fragments. At a distance, it appears as platy and bluish-red. It is less resistant to erosion than surrounding members.

pCs1 Lower quartzite member. Quartzite, dense, fine- to very coarse-grained, generally light gray, but commonly tinted yellow, light red, orange, which weathers to light reddish and various shades of brown. Abundant cross-bedding throughout the member. Ripple marks are common in the upper portion. Lenses of small well-sorted white quartz and jasper pebbles are present in the lower part. Locally contains lenses of dusky red to purplish-blue siliceous shale throughout the lower member, which is used to distinguish the lower member from the upper quartzite member. At a distance, it appears massive, and grayish to light reddish-brown. It is highly resistant to erosion and usually a cliff former.

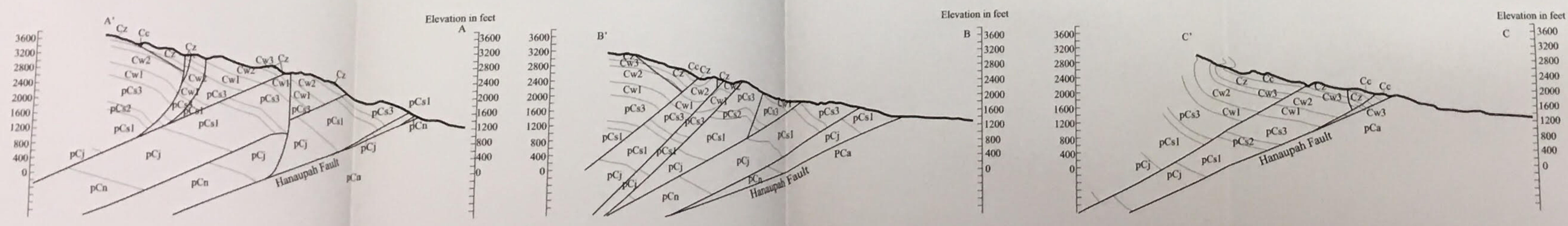
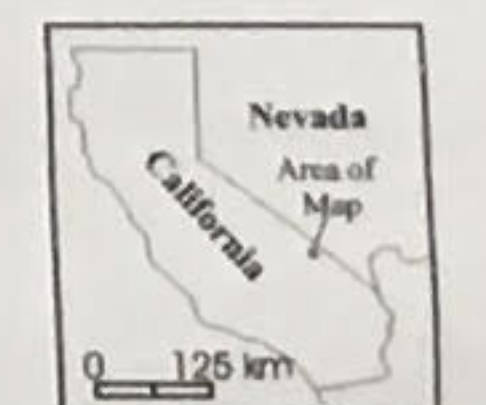
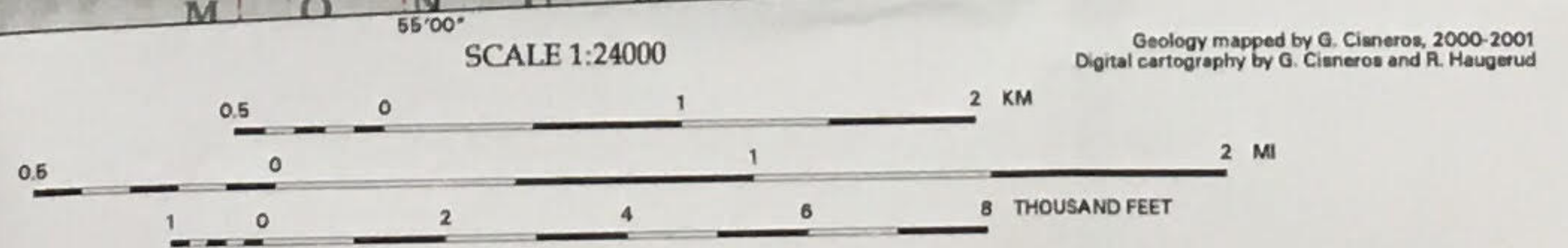
pCj3 Johnnie Formation (upper shaly member). Shale with thin beds of fine-grained quartzite and fine-grained dolomite. Shale is generally maroon and yellow to greenish gray. Sandstone and dolomite varies from brown to gray. In the western area, the upper portion this member consists of dolomitic sand that varies from coarse- to fine-grained.

pCn Noonday Dolomite. The lower portion consists of light creamy-gray, fine-grained dolomite. The rock is typically massive and thinly bedded. In weathered surfaces, the dolomite is grayish yellow in color and the unit is generally cliff forming. The upper portion of the Noonday consists of light creamy-gray, fine-grained sandy dolomite. It is generally poorly bedded and contains laminations and well-rounded to subangular fragments of white quartz and reddish jasper. The sandy portions weather to a rusty cream to brown color.

pCa Cataclastic Augen Gneiss

pCa Augen Gneiss. Basement rocks consisting of augen gneiss. Basement is intruded by numerous felsic dikes throughout the unit. Large dikes were mapped in the southern exposure of the basement rocks. However, the northern exposure of basement rocks consisted of such a high density of dikes that the dikes could not be mapped.

Base from U.S. Geological Survey 7.5-minute maps
Devils Speedway (1981) and Hanaupah Canyon (1987)
Albers projection, central meridian 120W
Shaded relief from USGS 10-meter DEMs
1980 magnetic declination = 14.5 deg E



Geologic map of the Hanaupah Canyon area, California
by
Gabriel Cisneros
2002